THE GEOMETRY OF CIRRUS BANDS AS RELATED TO METEOROLOGICAL CONDITIONS

- Part I: Text -

By

J.H. REUSS

Institut für Physik der Atmosphäre der
DEUTSCHEN VERSUCHSANSTALT FÜR LUFT- UND RAUMFAHRT E.V. (DVL), Außenstelle Darmstadt

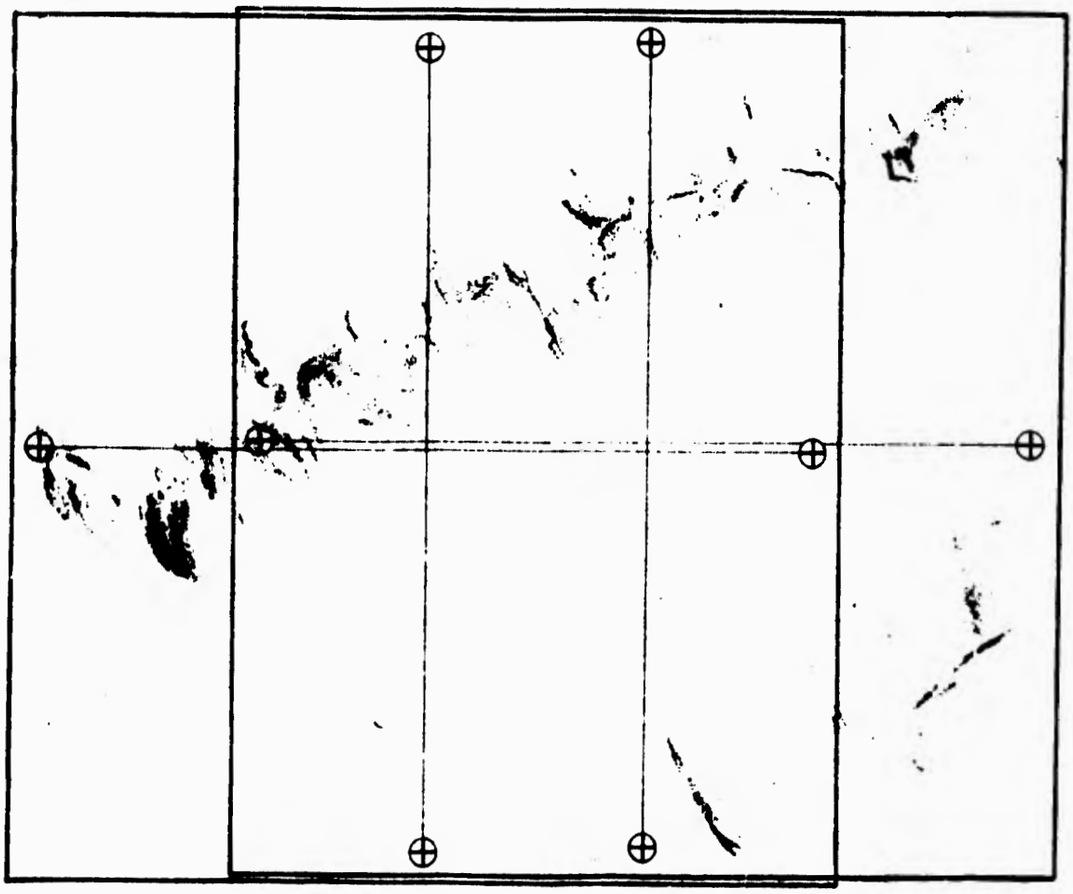

Final, Scientific Report
prepared for the EUROPEAN OFFICE OF AEROSPACE RESEARCH
of the AIRFORCE CAMBRIDGE RESEARCH LABORATORIES
under
Contract AF 61(052)-620 new
contractor: Prof. H. KÖSCHMIEDER
July 1964

THE GEOMETRY OF CIRRUS BANDS AS RELATED TO METEOROLOGICAL CONDITIONS

- Part I: Text -

By

J.H. REUSS

Institut für Physik der Atmosphäre der
DEUTSCHEN VERSUCHSANSTALT FÜR LUFT- UND RAUMFAHRT E.V. (DVL), Außenstelle Darmstadt

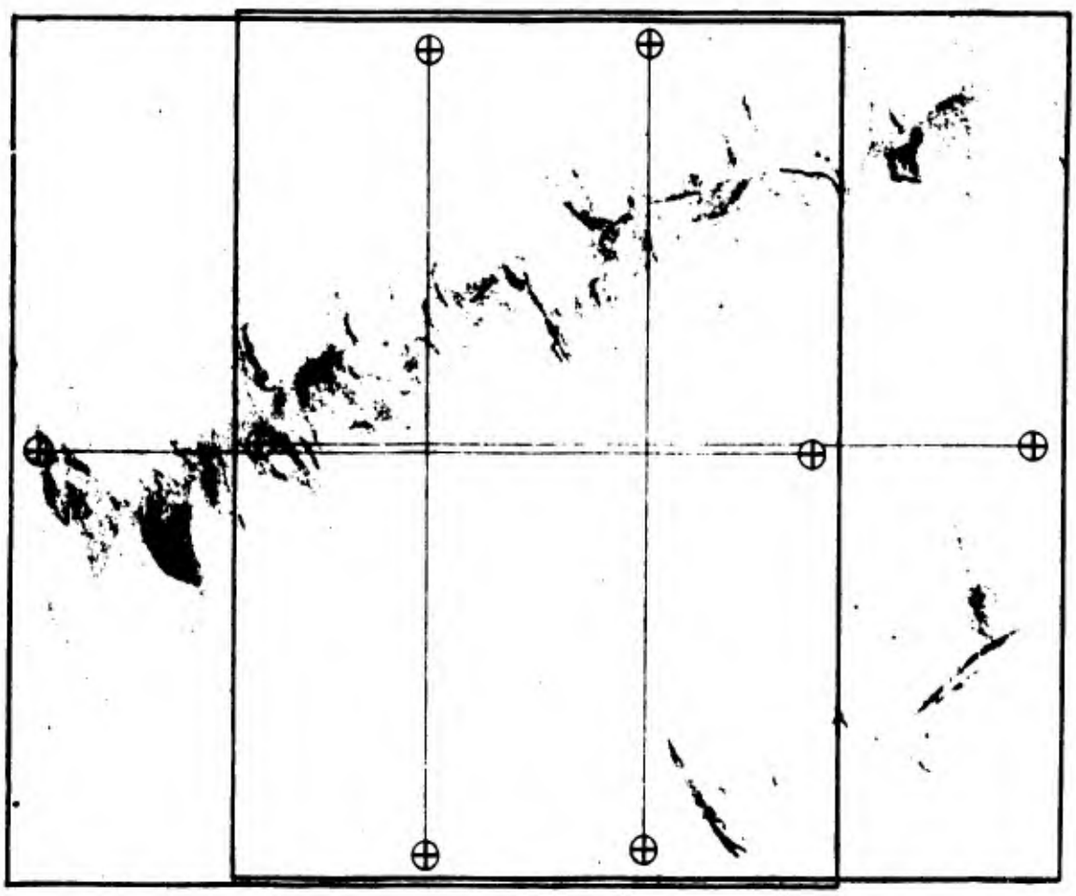

Final, Scientific Report
prepared for the EUROPEAN OFFICE OF AEROSPACE RESEARCH
of the AIRFORCE CAMBRIDGE RESEARCH LABORATORIES
under
Contract AF 61(052)-620
contractor: Prof. H. KOSCHMIEDER
July 1964

CONTENTS:

	page
Foreword	1
Summary	3
1. General-properties and definition of bands	5
1.1 Types of cloud "bands"	5
1.2 The phenomenology of cirrus band formation	8
1.3 Small scale lateral motion within ci-bands	9
2. Cloud bands as indicators of thermal wind at and directly below their level	12
2.1 Definitions	12
2.2 Wind profile necessary for band production	13
2.3 Band spacing	15
2.4 Thermal stability and other meteorological conditions which accompany ci-bands	16a
2.5 Anticipated causes of the band-isotherm parallelism, and discussion of a generalisation to other parameters	17
3. Statistical law governing the deviation of band orientation from the wind direction	19
3.1 Introduction	19
3.2 Wind shear statistics	19
3.3 Statistics of wind direction minus band orientation	24
3.4 Applications and further confirmation of $\Delta\alpha(|u|)$	
3.5 Causes of the $\Delta\alpha(|u|)$-behaviour	29
Appendix	32
(I) A brief account on the procedures of cloud photogrammetry	32
(II) An analogy to the $\Delta\alpha(|u|)$-law represented by a thought experiment	33
(III) Determination of the $\overline{\partial^2 u_r/\partial z^2}$ value	35
(IV) An account on the determination of vertical motion	36
Case study I : 13 May 1963	41
Case study II : 22 March 1957	55
Case study III: 6 Nov. 1962	62
Case study IV : 7 Nov. 1962	68
Case study V : 1 March 1963	76
Case study VI : 14 Febr. 1964	82
Literature	87

Foreword

This report summarizes the results obtained within two years of photogrammetric cloud studies mainly devoted to cirrus bands. These measurements aimed at determining the small and large scale behaviour of bands as related to the small and large scale state of the atmosphere -- the research of the large scale being done with respect to application for satellite picture interpretation.

With these objectives set it is obvious that this work is based largely on knowledge gained and detailed problems raised in recent years by CONOVER, KUETTNER, J.S. MALKUS, PLANK etc. The general conclusions laid down in the introducing chapters were drawn from a total of some 20 cases hitherto investigated as to both photogrammetric and meteorological data. Out of these case studies, six representative ones were selected for subsequent, detailed description in this report: The more pronounced the pattern of large scale cirrus bands is in the individual case, the more clearly do the accompanying meteorological conditions reveal their properties.

The precision photo theodolites used for taking the stereo photographs were designed and built in 1953 by ASKANIA/Berlin on the initiative of Prof. H. KOSCHMIEDER; they were sole paid by the SENATOR FÜR WIRTSCHAFT UND KREDIT of BERLIN from funds of the European Recovery Program (ERP). Since 1956 the taking of stereo pairs, gathering experience in all of the special work of cloud photogrammetry and subsequent research work, led by Prof. H. KOSCHMIEDER, have been financed by the DEUTSCHE FORSCHUNGSGEMEINSCHAFT (DFG). Also the stereocomparator, by which the coordinates are measured, is of DFG property.

The contract underlying this report meant a remarkable impact of problems and concepts, to the research done in Darmstadt. The contract monitor, Mr. John H. CONOVER, deserves our special gratitude for the problems he explained and the many suggestions he made in discussions, by his personal notes and in his publications.

Since Professor H. KOSCHMIEDER had retired in 1963 and, due to bad health, felt unable to carry on as contractor beyond July 1964, the contract, for formal reasons, had to be terminated before all the goals originally conceived were reached. Thus, the empirical part of this research fell short of local (Darmstadt) pibal soundings; however, for some 30 % of the cases and altitude intervals, they could be replaced by direct measurements of cloud motion vectors at different levels. These photogrammetric wind measurements estimatedly are of an accuracy up to the five-fold of pibal measurements. This is especially important for wind shear measurements. A more serious shortcoming was that in none of the cases stereo photography coincided with satellite passes coupled with picture readout. Cloud cover charts as composed of local observations are hardly a sufficient compensation since they do not clearly reflect large scale geometry of bands, while terrestrial photogrammetry, on the other hand, cannot exceed measurement ranges of some 200 km. Yet a few single picture sequences coincided with satellite photographs. Evaluations of both confirmed that the results obtained within stereo range are also valid for the large scale [22].

Thanks for their loyal assistance in working out this report are due to the following collaborators: Dr. Klaus WEGE of DEUTSCHER WETTERDIENST/Offenbach, made most of the synoptic analyses. His contributions to the results were signified as such; he has also reviewed this report. Mr. Rainer MEISSNER did most of the drawings underlying the Figures and contributed many an idea; he also read the proofs. Miss Marianne LUCZKA reproduced all the figures which necessitated photographic treatment. Mr. Fritz LEHMANN typed the first draft from the manuskript; finally, Mrs. Renate WAGEMANN typed the present fair copy.

Beside the contribution to this research with a share in funds of approximately one third by the DVL, by two third the research reported in this document has been sponsored by the U.S. AIR FORCE CAMBRIDGE RESEARCH LABORATORIES (AFCRL) through the EUROPEAN OFFICE OF AEROSPACE RESEARCH, UNITED STATES AIR FORCE.

Darmstadt, July 1964
Germany

The author

SUMMARY

The general results reported in here are based on a greater number of cirrus cases, some of which were not evaluated completely but merely to the extent as to answer special questions. The cirrus cases reported here represent some typical ones.

Large-scale cirrus bands, as defined under chapt. 1, were found to orient parallel with the large-scale isotherms at and some 2 km below their level : In most of the cases, ci bands generate above a layer of rather strong vertical shear, this shear decreasing (upward) toward band level without changing direction considerably. This strong-shear layer below ci-bands seems to be identical with a high-level front with the cold air lying below in most cases. In one case (IV), the cold air was above the strong-shear layer. There, bands generated within the layer of stong shear; the latter had a lapse rate close to dry-adiabatic. In any case, strong, large-scale vertical shear is necessary to generate large-scale ci-bands : The stronger the shear, the most pronounced are the bands generated.

A case of extreme vertical shear within slow winds else (case I), suggested to define a "thermal jet stream" (see Figs. 28, 29).

Small-scale lateral motion within the wings" of ci-bands, tending away from the band axis, was also measured; it was in fair agreement with results earlier obtained by CONOVER [6]. Band spacing close to regular was found in three cases (2 in case I, 1 in case II).

Another question to be answered was:

How is the direction of large scale shear -- and hence the band orientation -- related to the wind direction ?

An exploration of a great collective of

acute angles α_s enclosed between high-level shear direction and high-level wind direction, as well of

acute angles α between the motion direction and the orientation of cirrus bands

was carried out.

If we define $\Delta\alpha$ as the range of variation of both α_s and α (i.e. $0 \leq \alpha \leq \Delta\alpha$), and if $\Delta\alpha$ is substituted by $\Delta\alpha' = |\sqrt{\lg \Delta\alpha}|$, a relation between $\Delta\alpha'$ and the amount of band motion velocity, $|u|$, exists, which is fairly well approximated by

$$\Delta\alpha' \times |u| = c.$$

In this relation, $c \approx 38$ m/sec is constant for bands within altitudes 7 km $\lesssim z \lesssim$ 11 km and only within the tropopause, Toward lower altitudes, c decreases.

This relation implies that α may assume any value (i.e. $\Delta\alpha = 90^\circ$) at very small velocities, while it may not exceed, e. g.

$\Delta\alpha \approx 30^{\circ}$ with bands moving 51 m/sec; or

$\Delta\alpha \approx 20^{\circ}$ with bands moving 63 m/sec, etc.

It has to be emphasized, however, that while this relation is strictly valid for large-scale bands, it may not be strictly valid but yet yields a fair approximation for short bands or streaks (e.g. fallstreaks etc.). Since different geographical positions possess different long-term averages of high-level wind velocity -- e. g. the mean high-level wind over the area of Boston is greater than over the Darmstadt area -- the probability ψ that a band orients close to parallel with the wind direction also depends on the area where it occurs :

If $\psi_{20^{\circ}}$ defines the probability that the wind direction is within 20° of the ci-band orientation, $\psi_{20^{\circ}} \approx 0.7$ for the Boston area, but only $\psi_{20^{\circ}} \approx$ ≈ 0.3 for the Darmstqdt area.- Determination of $\psi_{20^{\circ}}$ for more areas of the world suggests itself in view of its eventual applicability to the interpretation of pictures taken by earth satellites.

The general description of these results is followed by a detailed description of six different cases of cirrus occurrence.

1. General properties and definition of bands.

1.1. Types of cloud "bands"

In order to obtain a survey on "bands" and to prepare a definition of the kind of bands which further interest is centered on in this report, we give a brief account on the phenomenology and modes of formation of various types of "bands".

This compilation does not claim completeness.

Billows and waves as such, which orient at right angle with respect to vertical wind shear, are excluded in advance.

(1) Streamers from (and caused by) an orographic obstacle. This kind of "band" and its cause has been described by LUDLAM and SCORER [12].

(2) Streamers which, also according to [12], originate if droplets freeze in the course of their passage through a wave cloud.

(3) Streamers induced by a rising cumulus cloud: As observed by the author, cumulus convection over an active source produced a narrow "street" of altocumulus, up to some 20 km in length downwind from the source. (The cu tops apparently did not attain altocumulus level; hence this case does not compare to an anvil).

(4) Single cumulus street, occasionally formed in the lee of an active convective source, according to [12]; in all cases observed by the author this source was provided by a hill top, heated by sunshine, which thus produced a local thermal instability.

(5) "Wave bands" (Fig. 1, from [10]). In this example of an altocumulus band of irregular width (average 5 km) and length ≈60 km, both ends of the band were quasi stationary; Despite a wind velocity of ≈38 m/sec at band level as determined by the fast travel of individual cloud points, the zone of "entrance" and of "exit" did not considerably alter their positions. The small scale bands which formed in the area of exit are discussed in chapt. 3.2.

This orographic source of this large scale wave motion could not be clearly determined -- its location was approximately 80 km in front of the entrance.

This kind of "band" has an ice cloud counterpart. A typical example, photographed by B. WOODWARD, has been described by KUETTNER [11]. While its entrance zone looks similar to that in Fig. 1, the exit zone will -- under similar conditions else -- be more remote from the entrance area, due to the delay associated with the eventual evaporation of ice particles.

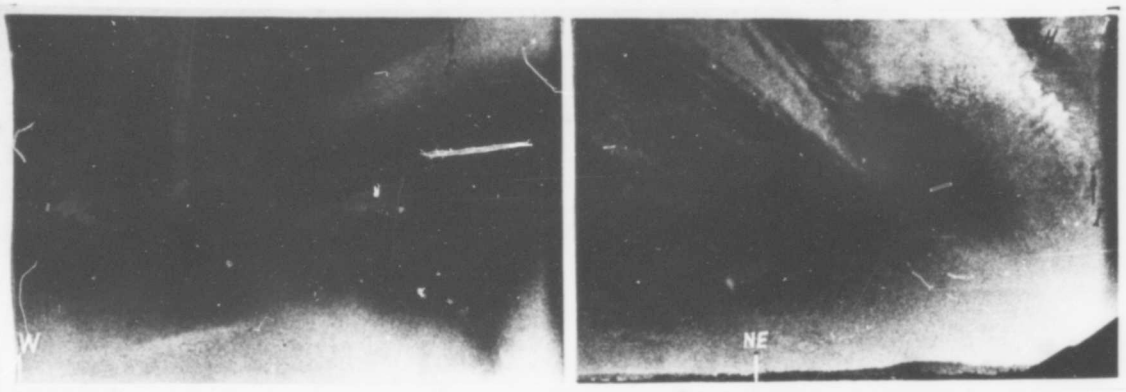

1a Entrance (left) and exit (right) of "wave bands", approximately 60 km apart. Note that the exit zone contains small bands (for comment, see chapt. 2.2).
Letters which denote points refer to a cloud map not shown here (see [10], case 10, of 12 Sept., 1962).

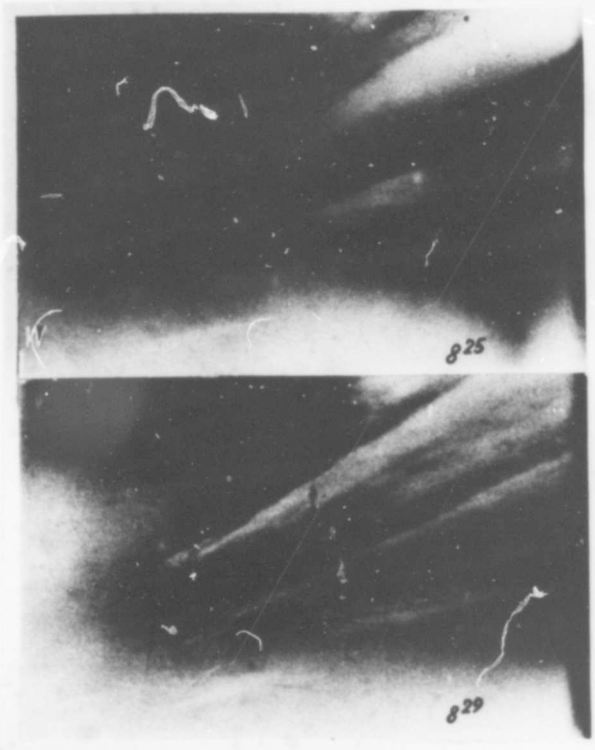

1b Migration of cloud point B within four minutes, with "wave band" entrance quasi stationary.

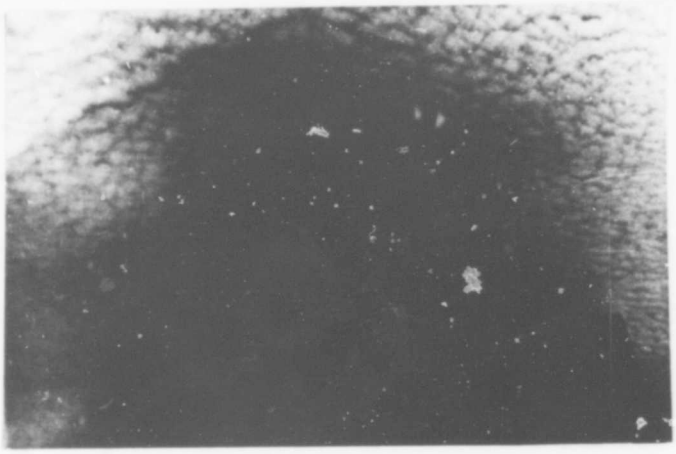

2 "Hole" in cc-layer, with faintly visible fall streaks; case of 14 Sept., 1962, described in [22].

3 "Hole band", approx. 15 m in diameter, in a very shallow ac-layer. Small scale vertical shear above layer anticipated.

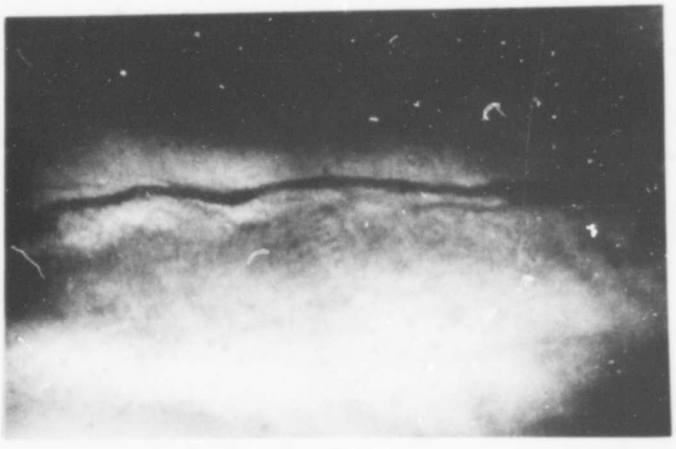

It is obvious that these trails -- represented by types (1) to (5) -- which form in the lee of some kind of source or obstacle, orient in the wind direction.

This is not always the case with the following kinds:

(6) "Bands" induced by an aircraft flying through a layer cloud of supercooled droplets, according to [12]. Naturally, they orient along the path of the aircraft. Since the orientation of these "bands" is not related to the properties of actual wind, it is proposed to call them "pseudo-bands". Results of stereophotogrammetric measurements of this kind of band were published in [10].

(7) Short "bands" which, according to LUDLAM, can be produced by fall streak regeneration (SCORER [24]); these bands will hence orient parallel to the wind shear which governs the fall streak orientation.

(8) "Hole bands". Holes of clear air which occur in layer clouds such as depicted in Fig. 2 (14 Sept., 1962, as described by REUSS [22]), occur in layers of practically no shear (similar, in this respect, to organized hollows; see CONOVER [8]). Correspondingly, "hole bands" originate in a layer of strong vertical shear: small scale hole bands (Fig. 3) occur in shallow shearing layers. A fine example of a large scale hole band is represented by a "crack" 1300 km of length, east of Madagascar, taken from TIROS I at 07:40 of 20 April, 1960. Large scale hole bands occur in large scale shearing layers and parallel the vertical shear. (For a definition of large and small scale shear, see chapt. 2.1). While cloud bands are produced by strong vertical shear in the layer below the cloud, hole bands may result from -- and hence indicate -- strong shear above.

Excellent photographs of single "holes" were supplied by BRUNT [3]. This author relates these single holes to a cell-producing BENARD regime. This interpretation has to be doubted, since a BENARD regime should produce neighboured, more or less organized hollows.

Correspondingly, single "hole bands" can hardly be assumed to be in analogy to an AVSEC convective regime.

(9a) Cumulus streets, also called "rows" [15], parallel mode [14] etc. From all the other "band" types hitherto described, they distinguish by the following features:

(α) Many streets create and exist simultaneously (for a more detailed description, see chapt. 1.2.); (β) they occur at the

same level, (γ) are oriented parallel to each other and of (δ) nearly constant spacing [11,14,15].

It is certainly justified, and in agreement with recent hypotheses both of KUETTNER [11] and J.S. MALKUS et al [14], to comprehend these cu-streets in analogy to the "longitudinal bands" defined and obtained by AVSEC's [1] well known experiments.

Upon suggestions of CONOVER [6] and KUETTNER [11] -- strongly supported by our results -- a close analogy also exists to cirrus bands [in our definition; see (9b) and subsequent chapters]. The results of our studies, which concentrate on ci-bands, may hence, in principle, be applied to cu-streets.

(9b) High altitude bands, of cirrus kind in most of the cases. Their appearance and occurance is close to that described under (α) to (γ) in the foregoing paragraph (9a). Hence these ci-bands also clearly distinguish from those briefly described under (1) to (8). Moreover, they are of large scale character as opposed, in general, to the "band" types of paragraphs (1) to (8). It is this category (9b) which we define as cirrus bands. Cases I, II, IV , V, and VI of this report represent typical examples; many more samples and discussion can be studied in the excellent work of CONOVER [6].

Prior to the description of their relation to wind and stability parameters, a more detailed phenomenology of their origin will contribute to the definition of ci-bands.

1.2. The phenomenology of cirrus band formation.

According to observations (e.g. case VI of this report) bands undergo (at least) three stages of development:

first stage: A more or less broad (≈1 km) band of haze becomes visible;

second stage: Within this band of haze, tiny white cloud spots ("cells") simultaneously come into existence; they are arranged along a nearly straight line.

third stage: While additional cloud spots join to form a broken -- but nearly straight -- line of cells, the more advanced ("older") cells spread laterally, creating "wings", toward both sides of the band axis. The cells born later continually follow this scheme.

The slow lateral motion of these "wings" and eventual preference of one of these sides due to small scale vertical wind shear[1] were first measured and described by CONOVER [6,7].

Further development may lead to a flattening of bands, e.g. growing into a stratus-like layer (cases II, VI).

Although this scheme of development may be not complete and in itself does not prove that ci-band formation behaves analogue to AVSEC's experimental model, it does prove that cirrus bands form by the same mode as cu-streets do.

A description of cu-street origin, given by PLANK [15] shows that cu-streets also obey the decisive second stage (as described above). KUETTNER [11] and PLANK [15] concluded that this stage must be preceeded by a band of increased humidity -- the latter being equivalent to the first stage in the scheme described above. This leaves no doubt that ci-bands as well are preceeded by humidity bands, at the top of which the bands form.

The somewhat organized small scale motion within bands as already mentioned, which is a vital part of their definition, will be described in the next chapter.

1.3. Small scale lateral motion within ci-bands.

According to AVSEC's interpretation of his well known experiments which produced "longitudinal bands", the existence of these bands is accompanied by a lateral motion best described as "helical" (e.g. CONOVER [6]). The suggestion that cu-streets and ci-bands are also accompanied by helical motion was first made -- to our knowledge -- by CLEM [5]. Later, on grounds of time lapse movie films as well as photogrammetric cloud measurements, CONOVER [6] stated that lateral spreading (away from band axis, toward both edges) takes place in both cu-streets and ci-bands, details of this motion depending on small scale vertical shear (see below); he suggested that this spreading represents the visible part of a helical motion. Our stereo-measurements in Darmstadt corroborated but hardly added to these empirical results. They may be summarized as follows:

---

1) For definition, see chapt. 2.1.

Appearance and small scale motion of these bands are in accordance with type (9b), chapt.11, and chapt. 2. The "wings" and "wing tips" which emerge from the "cells" toward both edges of the band are a few hundred meters (as a rule: 0.2 km) higher than the cells; in the symmetric case (see CONOVER [7], scheme Fig. 16a,c, or [6], Fig. 289 a,c); the lateral spr. ng of individual cloud points on the wings, toward both sides of the band axis takes place with a velocity $0.3 \lesssim v \lesssim 1.3$ m/sec each (cases I, II, VI, of this report). The width of the band, i.e. the lateral distance of the "wing tips" of a band, is in the order of 4 km, if (the axes of) two neighboured ci-bands are roughly 8 km distant from each other. A definite proof that helical motion would exist, represented either by a streamline or the path of an individual air parcel[1], appears to meet with difficulties as to both measurement and theoretical support:

(1) As to measurement: Within a coordinate system which travels parallel to the band movement but at a velocity which is approximately the mean[2] of (i.e. averaged across) the shearing layer (see chapt.2), a helical line reduces to a closed line. Its form is approximated by an ellipse lying in a sloped and slightly curved "plain". The path of an individual cloud point (within a "wing"), which is supposed to follow this line, may at best -- i.e. identifiable points taken for granted -- be traced and measured for 1 km[3]. In cu-streets it will be even less, since their "wings", as a rule, evaporate, and thereby loose identification, before they reach out considerably.

---

[1] Since this motion, taking place on a closed path, should be nearly stationary in a properly fixed coordinate system, we may replace streamlines by air trajectories.

[2] The exact determination of this velocity would necessitate a complicated mathematical procedure, the result being a function of the velocity component cross the band axis. This component is not known all over the path of the air parcel.

[3] For a band moving 20 m/sec at 10 km, a cloud area remains in the "visible" range of our zenit-directed stereo cameras for a maximum of 13 minutes. With a lateral point motion of 1 m/sec, this corresponds to a point path of some 800 m. *An investigation using smoke vanes as wind indicators -- measured by stereophotogrammetry -- ought to be tried.*

Hence this path, measurable at optimum conditions, corresponds to approximately 1/10 of one closed path along which an air parcel would follow in performing a helical motion. Taking into account, moreover, strong superimposition of random errors of measurement and point identification as well as random motion induced by turbulence, it becomes evident that within this range of measurement methods, no satisfying results can be obtained concerning this anticipated small scale motion.

A general theory of these motions will have to consider, among other facts, the heat released when the cloud comes into visible existence. Another question is: Which is -- with respect to the band -- the vertical position of the layer within which the helical motion takes place. There is reason to believe that for bands of equal spacing the boundaries of this layer are the same as the boundaries of the shearing layer described in chapt. 2.2.

In the next chapters, the relations of the orientation of large scale ci-bands to meteorological parameters will be of interest.

In order to obtain a plain survey on existing relations, it appears adequate to divide them into two categories beforehand:

(1) Laws which are valid without exception, thus being applicable to each individual case.
Laws of this category are discussed in chapt. 2.

(2) Statistical (or probability) laws, valid for a collective of a grater number of cases (or for the probability of an individual case). A relation of this kind is described in chapt. 3.

2. Cloud bands as indicators of thermal wind at and directly below their level.

Many cases, in which the orientation of cirrus bands deviated from their motion direction by angles up to 90°, led to the following, generally valid conclusion:

Large scale cirrus bands always parallel the isotherms of their own (and of slightly lower) levels[1].

This statement immediately calls for more detailed comments. In advance, this necessitates a discussion of atmospheric behaviour, introduced by the following

2.1 Definitions:

Large scale vertical wind shear must maintain an average amount of $\geq 6 \times 10^{-3}$ sec^{-1} and nearly constant direction throughout a shearing layer of vertical extent $\geq$1.5 km. Within this layer, this shear will -- on a probability basis -- be representative for

(1) a horizontal extent $\geq$150 km, with preference for the shear direction[2].
In a coordinate system fixed with respect to the mean wind in the shearing layer, large scale shear will also prevail for

(2) many hours (in the order of 10).

---

1) A preliminary result on this relation was reported in [20], and confirmed in [10]. If deviations of $\pm$ 10° are allowed for under a definition of "parallel", no exception of this law was found in the 15 stereo cases hitherto investigated. From a theoretical standpoint, small deviations due to ageostrophic affects appear to be possible. From the empirical standpoint, errors in isotherm orientations as determined from local temperature measurements, must be taken into account.

2) For a more detailed, quantitative treatment, the following kind of problem should be brought to a solution: A vertical wind shear, within a layer of thickness ΔZ in the troposphere and at high altitudes is assumed to be measured at a point where it has its horizontal maximum, s_{max}. A second variable is the horizontal distance d (as taken in the shear direction), at which the shear at the same level has decreased to $s_{max}/2$. Question: What is the most probable value of d as a function of s_{max}, ΔZ , and the mean stability within the shearing layer, and perhaps of additional variables.

Small scale vertical wind shear may attain and even exceed the amount of large scale shear; it is, however, restricted to a more shallow layer. If we arbitrarily confine the thickness of a shallow layer to be ≤ 0.3 km, the shear of this layer may be estimated to be representative for

(1) a horizontal extent in the order of $\lesssim 3 \times 10^1$ km -- more exact values depending on the degree of stability as well as on the amount of shear within the layer[1]; and for merely

(2) a few hours.

Relative wind[2] u_r at a level p_i results if we subtract the wind vector u_o, of the reference level p_o, from the wind vector u_i at level p_i (if altitudes $Z_i > Z_o$ and hence the pressure values $p_i < p_o$):

$$u_r = u_i - u_o.$$

In the following chapter 2.2., the reference level of the relative wind was chosen to be $p_o = 500$ mb.

2.2. Wind profile necessary for band production.

There is no doubt that to produce long ($\gtrsim$150 km) and pronounced ci-bands, large scale vertical wind shear is necessary. A review of the present and earlier measurement results [10, 21] has suggested that the band orientation is -- at least to a greater degree - governed by and parallel with the mean shear in the large scale shearing layer adjacent below the condensation level of the band. In other words, large scale ci-band orientation parallels (and hence indicates) the contours of the relative topography of a layer of $\gtrsim$1.5 km thickness, which is topped by the bands' tops.

---

1) see footnote 2) on page 12.

2) In techn. report No. 2 [22], it was denoted as "thermal wind". This expression has been abandoned since it does not in the strict sense mean the relative wind in a thick layer.

3) The degree to which bands are pronounced increases with the amount of vertical shear.

Due to its importance, the shape of the (relative) wind profile shall be described in more detail by a semi-quantitative scheme, in which the base of the shearing layer is arbitrarily chosen as 500 mb.

Starting at 500 mb, consecutive thermal winds 500→480 mb, 480→460 mb, ... 420→400 mb, will have approximately the same direction; therefore, all relative winds u_r up to 400 mb will have that same direction, their profile lying in a common vertical plane which is hence also oriented in that direction. (This vertical plane may, but not necessarily will, parallel the general wind direction). The shear amount is close to 15×10^{-3} sec^{-1} near 500 mb, and may decrease to 7×10^{-3} sec^{-1} near 420 mb. The condensation level of the bands, which orient parallel to u_r, will be close to 400 mb; at this level, as a rule, the vertical shear has decreased considerably or even ceased (Fig. 13 employs an example, but with a higher level).

This corresponds to KUETTNER's finding [11] that the condensation level of cu-streets is close to the altitude where the wind velocity has attained a maximum. PLANK [15] has also stated that at cu-street level the wind shear is strongly reduced, while it is great at lower levels.

Still higher, the vertical shear may remain small or continue in any direction, with preference for the opposite (180°) direction.

The profile just described well approximates that postulated by KUETTNER [11] for cu-streets. It represents, in general, the profile of the relative wind. In all the cases studied in here, $\partial^2 u_r / \partial z^2$ approximates the KUETTNER value, -1×10^{-5} $[m^{-1}\ sec^{-1}]$ (if u_r parallels the general wind direction, both sign and amount naturally apply also to the profile of the wind, whereby u_r can as well be replaced by u; for methods to determine $\partial^2 u_r / \partial z^2$ from actual u_r profiles, see Appendix, page 35). Whether this profile does accompany -- or even produce -- ci-bands as a consequence of the quasi-stabilizing effect which, according to KUETTNER, is induced by the profile, is a question beyond the scope of our research.

It is known from the settings of AVSEC's experiments [1] that both curved and nearly straight "wind" profiles produce longitudinal bands. In the free atmosphere, however, according to our

photogrammetric results, only less pronounced bands, or "bands" as described in chapt. 1.1., occur with a linear profile of the relative wind which would surmount the level of band tops.

2.3. band spacing.

From AVSEC's experiments it is known that band spacing is constant if the height of the layer is constant all over the vessel. Moreover, the ratio (spacing/height of layer) is nearly constant (≈ 2.5), increasing slightly toward greater dimensions.

If we disregard of eventual difficulties of applying AVSEC's results to the free atmosphere at all, thus assuming applicability in principle, we may state -- and draw conclusions from -- the following facts of experience:

Bands which come closest to regular spacing are cumulus streets. This is plausible, since their convective layer is enclosed between nearly "rigid" boundaries, of approximately constant levels: the earth or sea surface, and an inversion (or shallow layer of increased stability), according to KUETTNER [11], as well as to a few results on cu-streets obtained in Darmstadt.

In an altitude close to the tropopause, regular spacing which includes many bands, was observed in one single case (see case I, Fig. 7) with a spacing of only 2.2 km. These bands are most probably topped by an inversion or a shallow layer of increased stability, which was just below or even identical with the tropopause.

Another case of regular band spacing at high levels, though not pronounced to that degree, occurred within the band of a layer cloud (right part of Fig. 1a), taken from case No. 10 in [10]. It is evident from further discussion of these bands' origin (see chapt. 1.2.) that they owe their formation only to a decrease in stability, which

(1) followed few minutes after the cloud's origination,
(2) was limited to the thickness of the cloud layer, and was
(3) caused by radiation and evaporation at the top of the layer, and interception of the earth's radiation at the cloud base.

This development is analogous to that observed and interpreted by LUDLAM [12]: A few minutes past the formation of a thin sheet of layer cloud, small dapples create due to cooling at the top of the layer, caused by radiation of heat into space, while warming takes place at its base due to interception of the earth's radiation[1]. If we call this dappled type a BENARD regime, the banded type as described above should be denoted as an AVSEC regime (of longitudinal bands).

The presence of (small scale) vertical shear which creates these small bands, is revealed by the simultaneous appearance of small waves, which are roughly at right angle with respect to the narrow bands (see outer right of Fig. 1b, between points I and H).

This case of approximately equal spacing of narrow bands can be explained as follows: In view of the above hypothesis it suggests itself that the convective layer of this banding is nearly equal with the cloud layer[2]. If the ratio (spacing/vertical thickness of layer)$\approx$ 2.6, as found by AVSEC's micro-scale experiments, or if there is a somewhat different value of this ratio valid for clouds in the free atmosphere, then the thickness of the layer would be determined with known band spacing.

In all of the types of cases so far discussed, the convective layer was predetermined by pronounced boundaries: Earth or sea surface, strong inversion, tropopause, or the surface and base of a cloud layer.

Opposed to these, organized ci-bands, as a rule, display an only roughly equal spacing -- in most of our cases in the order of 10 km; it is often irregular with a spread (standard deviation) which is in the order of half the mean spacing (compare cases I, II,IV,V of this report). These cases, which represent a rule with ci-bands, suggest that due to lack of pronounced boundaries, the atmosphere "does not know" exactly which boundaries shall be valid as boundaries of the convective (or shearing) layer. In fact, the lower boundary is a more or less "blurred" high level front, as a rule (an exception represents case IV).

---

1) This is not the only way to create dapples; they were also observed, in patches of typical layer clouds, to create from the start, i.e. when the cloud came into existence [22].

2) These small, narrow bands thus do not form "originally", i.e. out of prior existing humidity bands.

2.4. Thermal stability and other meteorological conditions which accompany ci-bands.

Inspection of radiosonde measurements of the here presented and additional case studies did not reveal uniform values of thermal stability, if we define the latter as averaged over the thickness enclosed between the level where strong wind shear begins, and the level closely above band tops.
The decisive accompaniment, no doubt, is large scale shear, as defined before, linked with a horizontal temperature gradient of considerable amount.

The average lapse rate of ten band cases was $\left(\frac{\partial T}{\partial z}\right) \approx -0.77^{\circ}$/100 m (250/450 mb layer in U.S. Standard Atmosphere for comparison: -0.652°/100 m). But bands may occur at stability values which deviate considerably, toward both smaller and greater stability.

To explore the reasons for these different conditions, we include other accompanying meteorological conditions in the following survey.
We define

P_n as the normal to the paper plane within the frames at left of Figs. (a) and (b), page 17, these planes being parallel with the temperature gradient;

u_r as the relative wind, relative with respect to the lower boundary of the layer of strongest shear (at which, hence, $u_r = 0$; if vertical wind shear has constant direction within the layer, it parallels u_r).

Longitudinal sections, the position of which is marked by strong dash-stippled vertical line, are shown at the right of Figs. (a)(b).

u_r will always parallel P_n; both must roughly parallel (or more seldom: antiparallel) the wind direction, whenever the wind velocity is great at band level. In this case, the dashed, enclosed area at upper left is occupied by the jet core. Most of the cases reported by CONOVER [6] comply to this rule. *At slow wind, P_n may assume any direction (case I).*

Thermal stability within the layer of strong shear will depend on whether the cold air is (a) below -- which is the most common case -- or (b) above this strong shear layer, with a lapse rate within it close to dry-adiabatic.

Typical ci-bands will preferably form at type (a), such as described in case study II (with jet stream) and case one (with no jet stream); probably, case VI also belongs to this category.

Bands of more streaky appearance probably form under conditions described under (b), as represented by case IV. (This statement is still hypothetical since it is based on only one, moderately pronounced case).
The mean thermal stability in the layer between the lower boundary of strong vertical shear, and the level slightly above band tops, is greater in category (a) than under category (b).

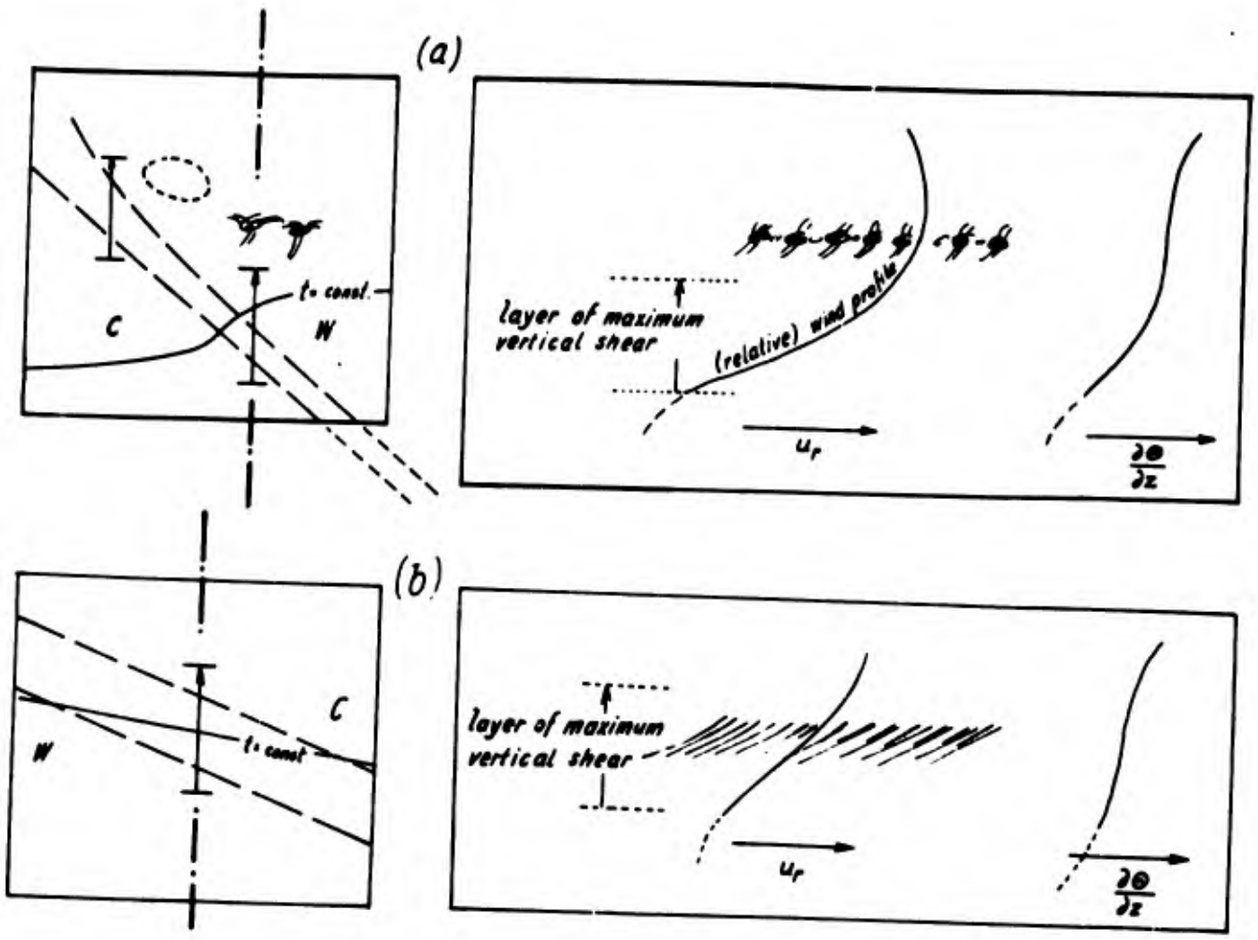

2.5. Anticipated causes of the band-isotherm parallelism and discussion of a generalization to other parameters.

There are reasons to believe that not merely wind shear itself causes large scale bands to parallel isotherms. Isopleths of additional parameters -- listed below -- also use to parallel them.

It was an idea of Mr. R. MEISSNER to chart isopleths of the temperature difference between two mb levels. The isopleths, which hence represent a measure of thermal stability, paralleled the isotherms especially well when the horizontal temperature gradient was great. This is plausible since the latter will in most of the cases represent a high level front. It is, therefore, suspected that even in a case of strong ageostrophic deviation of vertical shear from relative topography, large scale bands would rather parallel the isotherms than vertical wind shear. However, this assumption could not be made certain of since no case of marked ageostrophic deviation was encountered among the many cases so far investigated.

If we summarize

pressure (included, since isotherms lie on a p = const. level);
amount of vertical wind shear;
humidity;

cloud cover (as expressed by isonephs);
thermal stability;
R_i-number, or a different criterion for turbulent CAT;
large scale vertical motion, and
streamlines of vertical wind shear

under the denotation "atmospheric state", there is much empirical evidence -- in a pronounced manner represented by case I of this report -- that the statement of this section can be extended to the following hypothesis: Large scale, pronounced ci-bands parallel the isopleths of atmospheric state which prevail throughout the convective (or shearing) layer of the bands.

3. Statistical law governing the deviation of band orientation from the wind direction.

3.1. Introduction:

As early as 1896, CLAYTON [4] upon 1896 observations of cirrus bands over the Boston area which covered the time from 1889 till 1894, made the following statements (cited by KUETTNER, [11]): »" ... at all velocities the majority of bands lies in the general direction of their motion and but few at right angles to it; but the proportion of the bands which move in the direction of their length increases rapidly with the velocity. ... nearly 80 % of the rapidly moving bands (more than 100 knots) varied less than 23^{o} from the direction of motion." He also concluded that cirrus bands have the greatest mean velocity when moving longitudinally and the least when extending at right angles to their direction of motion.«

In this statistics, possibly two categories superimpose each other: bands and waves. But it is correct, as we shall see, regardless of this apparent superimposition, if we add that in cases of slow winds, any orientation is permitted for both bands and waves[1].

3.2. Wind shear statistics:

To obtain a survey on the statistical relation[2], we tried to reconstruct the actual relation. Beforehand, there were not enough band cases available for an extensive collective [20].

Applying the law of chapter 2, band orientation could be replaced by the mean of shear orientations within a layer of constant thickness; this enables to obtain a collective of a large number of cases.

The deviation of the mean vertical shear, of 400→300 mb and 300→200 mb from the 300 mb wind is being defined by the acute angles α_1 and α_2, respectively, according to Fig. 4.

---

[1] According to SEKERA [25], waves may occur only in moderate vertical shear.

[2] Also, since we did not possess the original publication of CLAYTON.

The mean deviation is defined as

$$\alpha_s = \frac{1}{2} (|\alpha_1| + |\alpha_2|). \qquad (1)$$

For a first experiment, 174 days with either small or great wind velocities had been chosen by inspecting the weather maps. The wind data of routine aerologic ascents of those days were used to determine the respective α_s values. Concept, method and results have earlier been described [20].

An improved method, employed later [10], considers also the amount of wind shear; it is as follows:

From the data of aerologic ascents from one station (i.e. Stuttgart and/or Emden), α_s is calculated (from graphical charts of the kind of Fig. 4) for a number of days which is great enough for statistical evaluation. Fig. 6 depicts 330 values of α_s versus the corresponding value of the velocity u at the 300 mb level. The diameters of the full circles are proportional to the mean amount s of the mean vertical wind shear amounts s_1 (between the 400 and 300 mb level) and s_2 (between the 300 and 200 mb level; for scale of s, see upper right of Fig. 6). A correlation of u versus s has been shown in [10].

The method still bears the following disadvantages:
The values α_s and s (and u) are not precisely known since (1) the underlying wind data are relatively inaccurate as to both direction and velocity (REITER, [19]); (2) wind data are too sparse as to allow for the systematic use of levels closer to 300 mb for the determination of neighboured vertical shear (which would allow for a different, more detailed definition and determination of α_s); (3) if the wind maximum lies within 400 to 200 mb, the case of Fig. 5a will not be the rule (wind directions were arbitrarily chosen as 260°, 280° and 280° for 400, 300, and 200 mb respectively); instead, in the general case, maxima or minima will occur neither at 300 nor at 400 mb, as shown in Fig. 5b. If, in addition to the above mentioned equ. (1), we define α_s' as the mean angle of deviation of vertical wind from the direction of the maximum wind, and s' as the mean amount of the shear vectors neighboured to the maximum wind, it becomes evident that $\alpha_s \geq \alpha_s'$ and $s \leq s'$. This means that, even at great velocities, α_s may reach or even exceed 45°; this has to be kept in mind in judging Fig. 6. However, toward an increasing number of cases, an asymptotical approach toward the true statistical behaviour would result.

The same statistical scheme should be obeyed by the acute angle α between wind and band orientation, since the latter are linked to wind shear. This, indeed, proves to be true (Fig. 7).

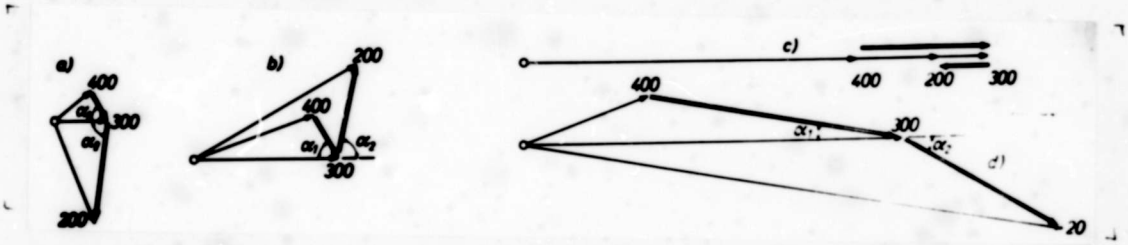

4 Definition of α_1 and α_2 as acute angles between the 300 mb wind and the mean vertical shear between 400 and 300 mb , and 300 and 200 mb, respectively . Cases a and b prevail at calm, cases c and d prevail at strong winds.

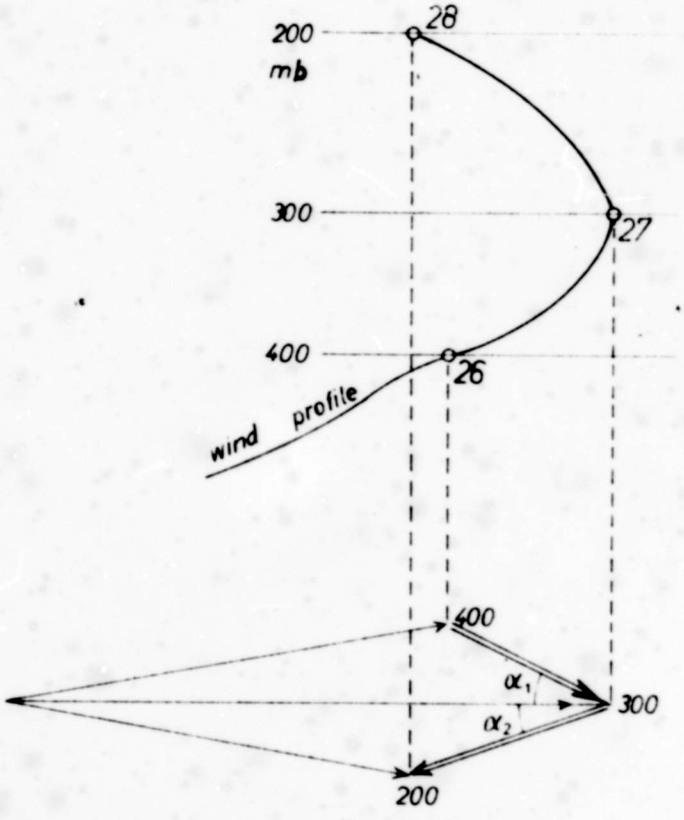

5a Wind profile and resulting α_1 and α_2 it the wind maximum is at 300 mb.

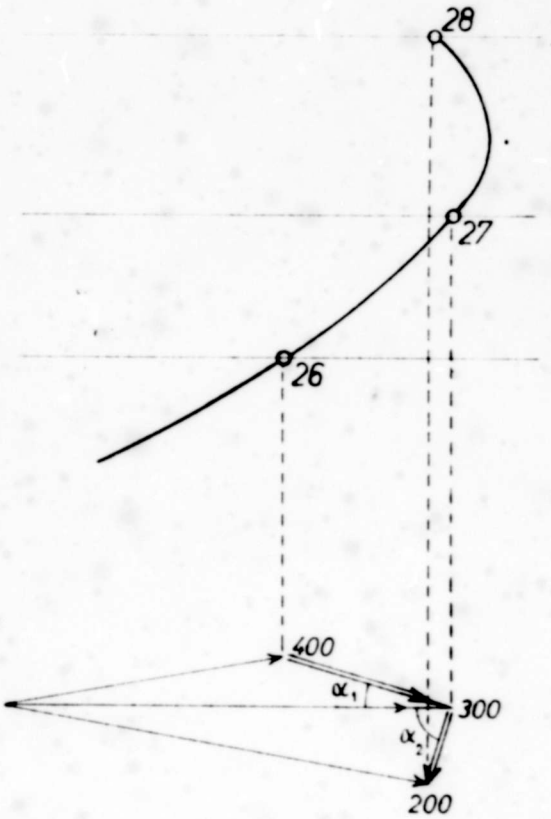

5b Wind profile and resulting α_1 and α_2 , it the wind maximum is between marked millibar values.

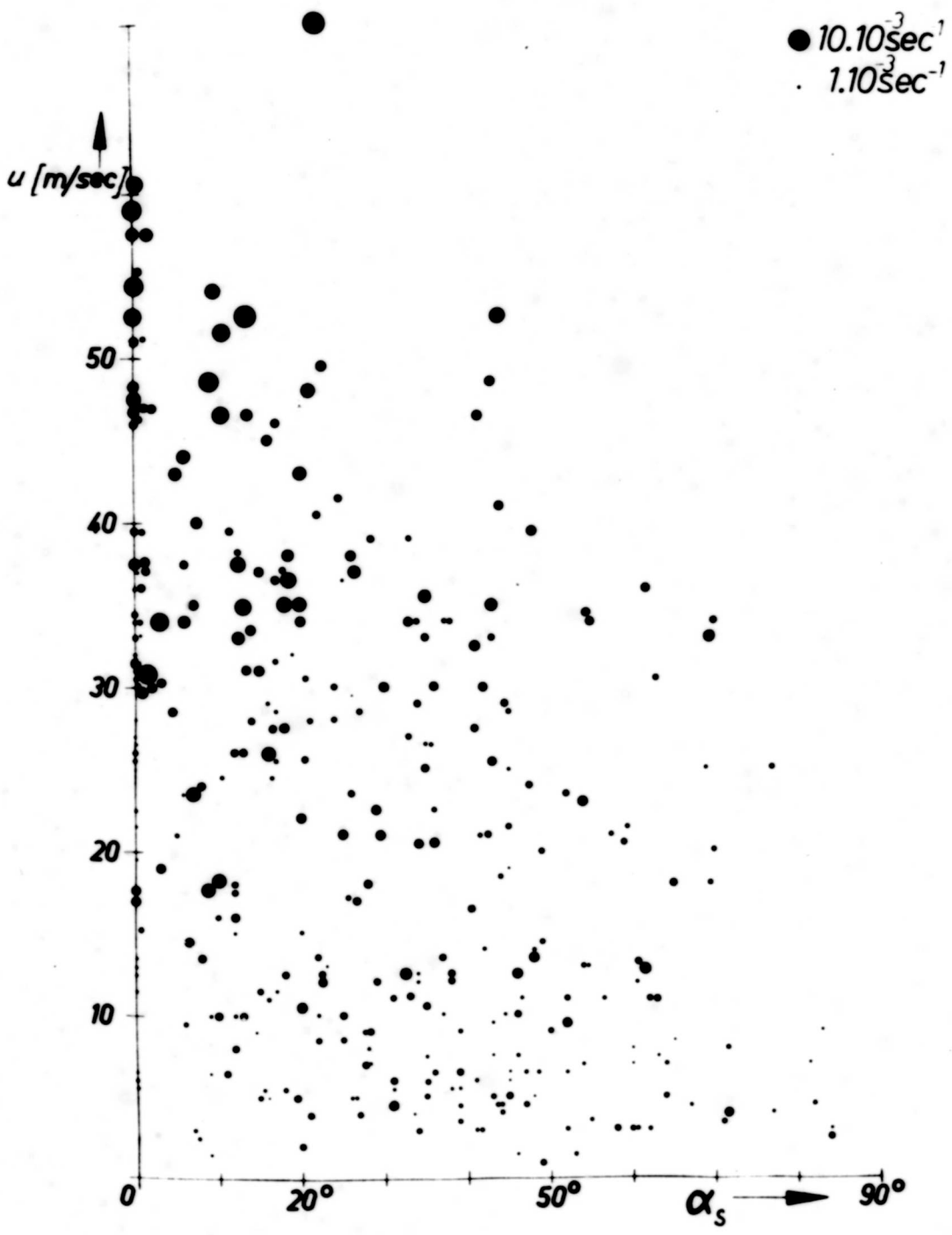

6 330 cases of α_s versus 300 mb wind velocity. Vertical shear values proportional to dot diameters (for scale, see upper right) .

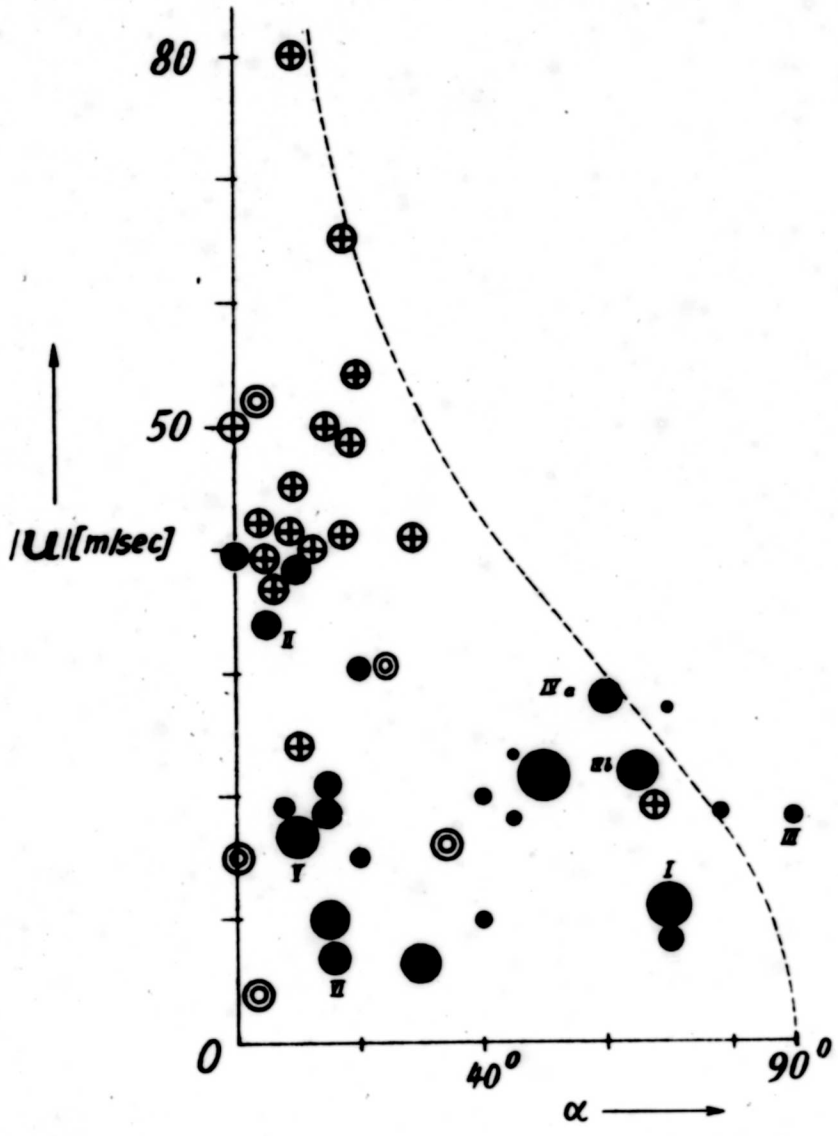

7 α(|u|)-statistics: Each point represents an individual case of ci-bands at levels > 7 km, analyzed as to their motion velocity |u|, and the angle α by which their orientation deviates from their motion direction. This graph includes
16 cases of large scale ci-bands as measured 1956/59 by CONOVER near Boston (⊕);[1]
5 cases of ci-bands ("polar bands" as they were called), as measured 1896/97 by SÜRING near Berlin (◎); and
24 cases of ci-bands and streaks which occurred near Darmstadt 1957/64, ● including small bands and streaks, and
1 case of ci-banding near Kniebis, 1956 ●.
Diameters of full circles in [mm] equal the third root of the lengths [km] which the bands at least had.
The cases I to VI were included in this statistics and denoted by their respective number.
The huge circle below IVa means a ci-band depicted in a satellite photo, hence revealing the band's full length [22].

1) Of case Nos. 1, 4, 5, 6, 7, 9, 13, 14, 16, 17, 18, 19, 22, 23 [6], in which ci-band altitude ≥ 8 km.

7.3. Statistics of wind direction minus band orientation.

Beside results obtained in Darmstadt, this statistics includes results obtained by CONOVER in 1956 to 1959 [6] at Blue Hill Observatory, and by SÜRING in 1896 to 1897 [26] in Potsdam. Their results were introduced into this statistics not only because the cases measured in Darmstadt were considered too small in number,

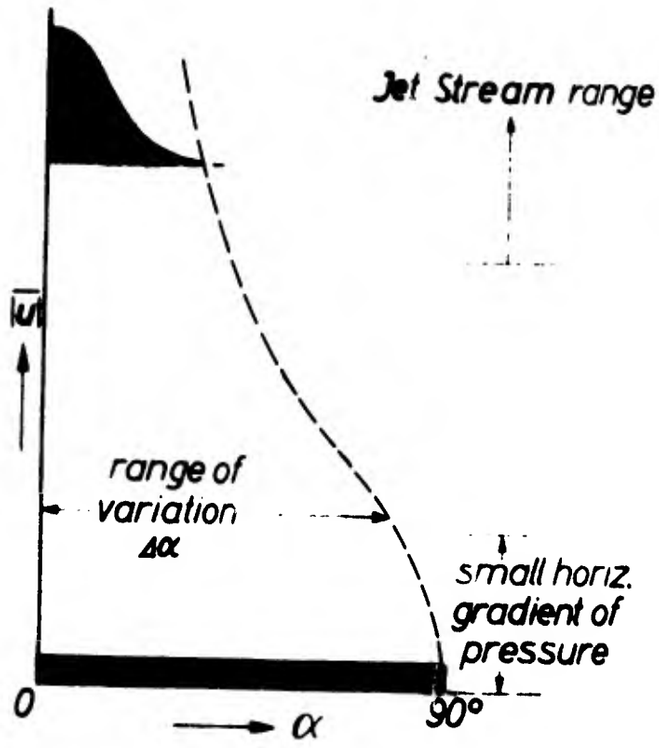

8 Anticipated relative frequency distribution of α. The relative frequency (hatched) is evenly distributed at calm air, but would obey a Gaussian distribution at rather great wind velocities.

but also because of the much greater wind velocities associated especially with the bands measured by CONOVER [6][1].

The graphical statistics (Fig. 7) thus contains: 16 cases of ci-

[1] In Central Europe, great high level wind velocities not only occur far more rarely than in northeastern USA, but also are almost invariably accompanied by low clouds which prevent continuous photography of eventually occurring high level cirrus bands.

bands measured by CONOVER, their altitudes exceeding 8.0 km; the (only) 5 stereo cases of "polar bands" of an altitude > 8.0 km measured by SÜRING [26]; and a total of 24 bands and streaks at altitudes > 7 km measured in Darmstadt (for more detailed information, see below Fig. 7), which add up to 45 individual cases.

Defining

α = acute angle between band orientation and band motion (the latter equal to the wind direction at band level);

$\Delta\alpha$ = range of variation of α, within a greater number of band cases of approximately the same motion (= wind) velocity (see Fig. 8), and

$\Delta\alpha' \equiv |\sqrt{tg\Delta\alpha}|$,

the range of variation of α, as found empirically, can be approximated by

$$\Delta\alpha' \approx |\mathbf{u}| = c. \qquad (2)$$

For bands within an altitude range of $7 \leqslant z \leqslant 11$ km, $c \approx 38$ [m/sec][1]. In Fig. 7, equ. (2) is represented by the dashed line. It will be noted that it also approximates the wind shear statistics (Fig. 6) -- taking into account the above described weaknesses of the method underlying the latter.

In the shear statistics (Fig. 6), 4 % of the points lie beyond the line defined by equ. (2); in the band statistics it is 5 %.

The principle of this band statistics has also been found to apply to HELMHOLTZ waves of mesoscale horizontal extent (REUSS, [22]). Since waves orient normal to vertical wind shear, the normal of the waves is the direction which in case of a wave statistics substitutes the band orientation, in the statistics.

With an increasing number of cases summarized in this statistics, the latter will asymptotically approach a long term average distribution. Its relative frequency distribution is assumed to equal that of Fig. 8.

Since the long term average of high level wind velocity, $\overline{|\mathbf{u}|}$, is known to depend on the geographical position, it follows from the $\Delta\alpha(|\mathbf{u}|)$ relation that the mean value $\bar{\alpha} = \sum^{n}\alpha/n$, must also be related to geography[2].

---

1) $\approx$ denotes "approximately"; at lower altitudes, c has smaller values.

2) It is evident from Fig. 8, that $\bar{\alpha} \leqslant \frac{\Delta\alpha}{2}$.

Since α and α' are related, $\Delta\alpha'(|\mathbf{u}|)$ establishes also a function $\Delta\alpha(|\mathbf{u}|)$, which will further be employed.

3.4. Applications and further confirmation of $\alpha(|\mathbf{u}|)$.

3.4.1. The mean value of α as related to geography. As was mentioned in the foregone paragraph, high level wind velocities are generally greater in northeastern (n.e.) USA than over Central Europe (C.E.). From a random test including 100 days each, the mean value of 500 mb wind velocities, $\overline{|u|} = \sum |u|/n$, was calculated for Berlin and for Boston (or nearby stations), respectively. Results were, for Berlin: $\overline{|u|} = 18$ m/sec; Boston: $\overline{|u|} = 27$ m/sec. Since we must confine to days at which long bands would occur[1], hence associated with strong, large scale shear, and to levels higher by $\gtrsim 2$ km, the corresponding average velocities of band motion (= wind) will exceed the average values just mentioned. With this in mind, it is plausible that actual measurements by CONOVER at Blue Hill yield $\overline{|u|}_b \approx 45$ m/sec, while the Potsdam and Darmstadt data yield $\overline{|u|}_b \approx 20$ m/sec. This enables to reason that these values come close to the real long term average velocity of days with band occurrence. Correspondingly, band cases occurring in the Boston area will generally occupy mainly the upper (and hence left) "area" in Figs. 7, 8; whereas band cases in C.E. occupy the lower portion of the graph, causing a broader distribution. Hence the average $\bar{\alpha}$ as well will represent roughly the long term averages. The case studies of CONOVER yield $\bar{\alpha} \approx 20^\circ$ for n.e. USA, against $\bar{\alpha} \approx 40^\circ$ for C.E. as derived by the cases measured in Potsdam and Darmstadt.

Since the probability Ψ for $0 \leq \alpha \leq 90^\circ$ must be $\Psi = 1$ (by definition of α), Figs. 6,7,8 enable to derive rough values of the long term average probability that the wind direction keeps within (an acute angle of) 20° of ci-band orientation[2]. This probability is $\Psi_{20^\circ} \approx 0.3$ for C.E., while for n.e. USA it amounts to $\Psi_{20^\circ} \approx 0.7$.

As the reader will note, these Ψ_{20° values are valid for any large scale ci-band regardless of its individual motion velocity (i.e., Ψ_{20° is velocity-independent); however, changes in the local mean velocity

---

[1] This naturally includes bands not visible from surface due to lower clouds.

[2] The well known 180°-ambiguity can in most cases be excluded from judging the neighboured weather situation;

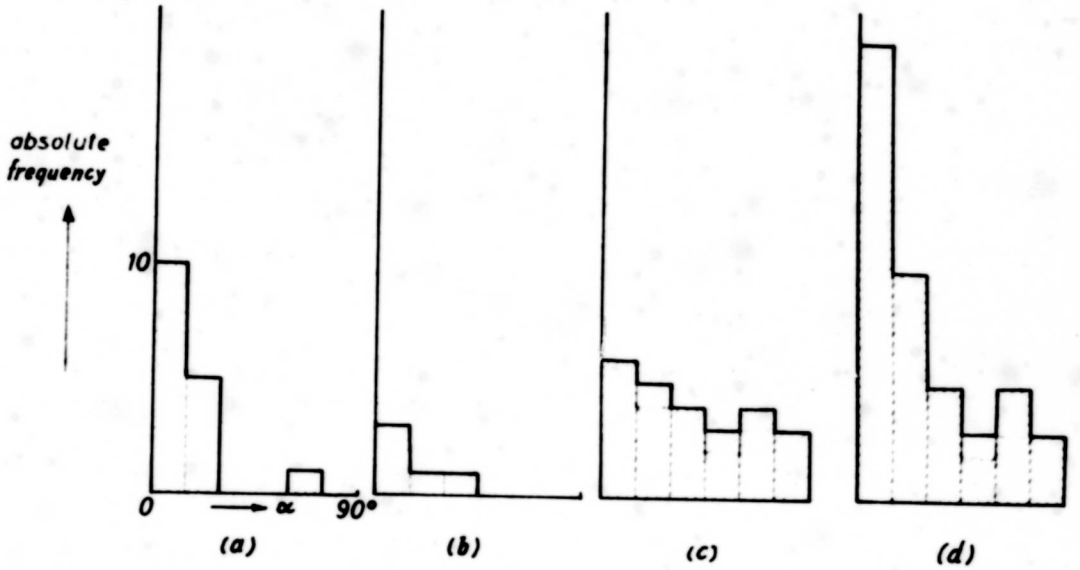

9 Absolute frequencies of α in 15°-intervals, versus α, of ci band cases at
(a) great average motion velocity (16 cases of CONOVER [6];
(b) moderate " " " (5 " " SÜRING [26], not very representative due to small number of cases;
(c) small average motion velocity (24 cases which occurred at Darmstadt and Kniebis;
(d) total of (a), (b), (c),
as deduced from Fig. 7.

due to seasons and long period weather situations, should be accounted for.

The absolute frequency distributions of α as derived from Fig. 7 for different places of measurement, and divided into 15°-intervals, are depicted in Fig. 9.

It suggests itself to determine long term mean values -- breaking down into seasonal means -- of high level winds as well as the resulting Ψ_{zo} values, of more areas of the world (and to compare these to routine pibal and satellite-photograph measurements).

A similar relation results if we apply $\Delta\alpha(|\mathbf{u}|)$ to one single large scale system of bands extending in areas of very different wind velocities (Fig. 10)[1]. Evidently, the "onset" of strong vertical

[1] To characterize the situation, a somewhat exaggerated picture was used. However, in rare cases such as case 1 of this report, even more pronounced situations of this type occur.

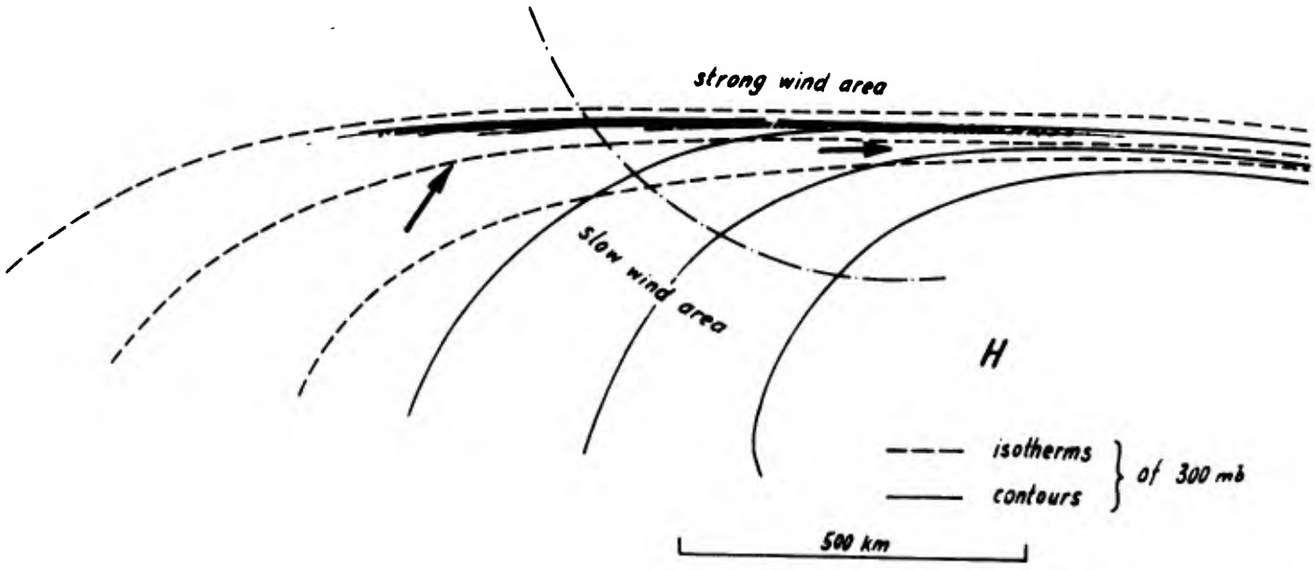

10 Isotherms parallel contours in area of strong wind.

wind shear caused by a great horizontal temperature gradient ("thermal jet stream") still lies in the slow wind area located in front of the jet stream entrance. For that portion of the band which is located in this area of slow wind, the probability is comparatively great that its motion component cross the band orientation still has a considerable share of its motion vector. Opposed to this entrance position, the major portion of this band travels at greater velocities and into a direction nearly parallel to its orientation.

This touches the question as to the causes of the $\Delta\alpha(|u|)$ statistical behaviour. Attempting an explanation calls for merely atmospheric aspects.

3.4.2. Large scale isotherm patterns as related to streamline patterns of the wind. As a consequence of the $\Delta\alpha(|u|)$ relation, isotherms -- at least at high levels --, of an area of great extent should also tend to parallel contours toward increased wind velocities. To encertain of this behaviour, 300 mb contours and isotherms of 60 days of the area of Germany were charted. By these charts, mean acute angles α_i between both line patterns, and mean horizontal pressure gradients, $\bar{g}$[gpm x km^{-1}], were determined. From a total of 8 points at $\bar{g} > 50 \times 10^{-2}$ (corresponding to great wind velocity) $\bar{\alpha}_i = 16^o$ resulted; while for 27 points at $0 < \bar{g} \leqslant 30 \times 10^{-2}$, an average $\bar{\alpha}_i = 42^o$ was obtained.

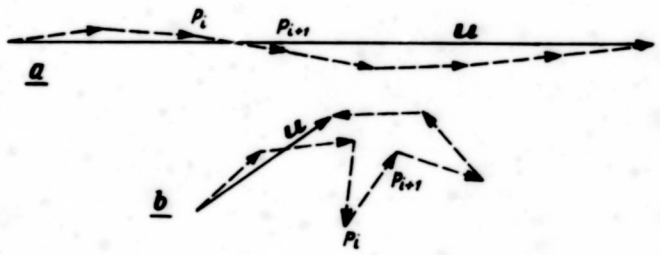

11 Two different types of addition of thermal wind vectors.

3.5. Causes of the $\Delta\alpha(u)$-behaviour

may at least be twofold: (1) In terms of wind and thermal wind: We anticipate the existence of thermal winds 900→850 mb, 850→800 mb, ... $p_i \rightarrow p_{i+1}$, ... , 300→250 mb, which all possess approximately the same amount of vertical wind shear (of the order 10^{-2} sec^{-1}). If we disregard of the surface wind and of friction and eventual ageostrophic effects, the thermal winds add up to the actual wind (Fig. 11).

In case (a), with all thermal winds having nearly the same direction, the resulting actual wind will be (1) nearly parallel with the thermal wind close to its level[1], and (2) of great amount.

In case (b), with a "random" addition of thermal wind vectors, the resulting actual wind will in general (1) differ from the thermal wind direction by greater angles, and will (2) be of comparatively small amount. The latter effect is often still increased since case (b) will, as a rule, be associated with smaller amounts of thermal wind vectors.

Type (a) of this cause (1) seems to be associated mainly with a jet stream, the stream lines of which are nearly straight for at least 1000 km.

---

1) Small shear vectors directed nearly at a right angle to the prevailing shear are sometimes encountered. They use to occur within stable layers which are too shallow as to have an influence on large scale band orientation. Thus, the existence of these "normal" shears is reflected merely by falls streaks directed, correspondingly, more or less cross the large scale band orientation.

(2) A low level wind of relatively great velocity will, correspondingly, be accompanied by a relatively great, large scale horizontal wind shear. Whatever pattern the upper level isotherms may have at the beginning, they will be subject to deformation by this lower horizontal wind shear. This deformation may be modified directly, and (indirectly:) by the deformation of large areas of ascending and descending air movement. (However, cause and effect may, to a degree, exchange roles). The stronger the wind and hence the horizontal shear at lower levels, the more will the resulting deformation tend to orient the isotherms parallel to the streamlines of the general flow; this, in turn, reinforces or -- depending on the direction of the temperature gradient -- slows the wind velocity, adding to the horizontal shear, etc.

A well known example is the behaviour of upper level isotherms over a Low, from its birth at lower levels, to its occlusion stage.

There may be interaction between these two and, eventually, additional causes, such as turbulent "friction"[1]; also, altering amounts of the thermal winds have to be considered; therefore, this explanation may not be complete.

At any rate, an interaction exists between the roles of cause and effect. The statistical relation $\Delta\alpha(|u|)$ therefore primarily means that great u and small $\Delta\alpha$ accompany and condition each other to the effect that $\Psi_{i\sigma}$ amounts may be derived from local long term mean velocities. (It should, however, not be understood strictly in the sense that quite in general great u would cause small $\Delta\alpha$).

4.5. An application to vortex patterns.

In addition to the individual band cases described in this report, which certainly represent portions out of still more extended patterns, the patterns of large scale vortices, which mainly consist of lower clouds, should also conform to the relations herein described.

Recently, an Atlantic vortex pattern[2], which was not related to a

---

[1] rather quasi friction, since it is mainly caused by inertia forces.

[2] depicted by TIROS IV on 45th orbit, 11 Febr., 1962, at 16:30; vortex center was near 37°N, 40°W.

Low but to a cold air drop in the 500/1000 mb relative topography, was found and discussed by BUSCHNER [2]. This vortex pattern was not pronounced to the degree which vortices associated with a Low -- especially in its occlusion stage -- usually display; also, the vortex center was distant from the center of the cold air drop by 400 naut. mi. (where the time interval of 4.5 hours between the measurement of both was taken into account). This may to an extent be due to the very small number of -- and great distance between -- aerological ascents available for the vast area.

We agree with the assumption [2] that the cloud bands which "converge" into the vortex center are certainly related to the actual thermal wind field induced by the cold air drop.

BUSCHNER [2] anticipated that a cold air drop which -- like this one -- is not associated with a high-reaching Low, would occur "... only at comparatively small horizontal temperature gradients within a field of comparatively strong horizontal pressure gradients ...". Plausible as this appears at the first glance, it does not comply with our results (e.g. cases I, IV, and others not published here): Especially in case study I severe large scale vertical shears opposite to the low level wind compensate the latter to the effect of rather weak high level pressure gradients; -- or rather because of this -- a cold air drop with strong horizontal temperature gradient hardly reflects in the contour pattern.

On the other hand, the $\Delta\alpha(|u|)$-statistics complies well to the conditions which accompany this vortex: Since the latter in this case implied α which are great in general, $\Delta\alpha$ will be close or equal to 90°. According to $\Delta\alpha(|u|)$, this may occur in a region of weak horizontal pressure gradients. This is in fact the case with this vortex and the cold air drop, since they occurred in that area of a High ridge where the horizontal pressure gradient -- as an inspection of the 850, 700, and 500 mb contours showed -- had a minimum.

In the case of another large vortex,[1)] a considerable portion of its large bands (apparantly at 700 mb) moved cross their orientation. An investigation of the accompanying meteorological conditions showed :

(1) Bands were everywhere parallel with the rel. topography 700/1000 mb;
(2) The angle between wind and band orientation decreased in an area where the wind velocity was greater.

1) Tiros I
5 Apr. 1960
30°N, 145°W

APPENDIX

(I) A brief account on the procedures of cloud stereo photogrammetry.

Terrestrial stereo photogrammetry, as applied to clouds, has a moving target as an object of measurement. This often calls for a taking direction other than that of the normal case[1]. Thus, in addition to a vertical tilt α (with respect to the horizontal), and a simultaneous horizontal tilt φ - - with respect to the base-line normal - - may become necessary. A small deviation $\Delta\varphi = \widehat{\psi}$ from parallelism should also be accounted for.

Since the evaluation is done in the stereo comparator, all degrees of freedom other than the picture coordinates x', y', $p_{x'}$, must be expressed by a formula. With the additional variables α, φ, $\widehat{\psi}$, the distance of a cloud point from the plane of the photographic plate of the left stereo camera is

$$y = \frac{b}{p_{x'} - c'\widehat{\psi}\left(1 + \frac{x'^2}{c'^2}\right)}\left[c'\cos\left(\operatorname{arctg}\{\operatorname{tg}\varphi \cdot \cos\alpha\}\right) - \left(x' - \left\{p_{x'} - c'\widehat{\psi}\left[1 + \frac{x'^2}{c'^2}\right]\right\}\right)\sin\left(\operatorname{arctg}\{\operatorname{tg}\varphi \cdot \cos\alpha\}\right)\right]$$

$$\text{with} \begin{cases} b = \text{baselength} \\ c' = \text{focal length} \\ p_{x'} = \text{horizontal parallax} \end{cases}$$

The system of coordinates in which a cloud point shall be determined, is arranged as follows : The projection of the photographic axis of the left camera on the horizontal plane is the Y- axis, within the horizontal, at right angle with respect to Y, the X- axis is positive toward right, the Z — axis points toward zenit.

With $z = \frac{z'}{c'}\,y$, $x = \frac{x'}{c'}\,y$, the coordinates are

$$Y = \begin{vmatrix} y & z \\ \sin\alpha & \cos\alpha \end{vmatrix}, \quad Z = \begin{vmatrix} y & z \\ -\cos\alpha & \sin\alpha \end{vmatrix}, \quad X = x$$

In the normal case ($\varphi = 0$), with horizontal photographic axes ($\alpha = 0$) and precisely parallel photographic axes ($\widehat{\psi} = 0$), the above system reduces to the well known formulas

---

[1] "Normal case" - - a technical term in photogrammetry - - means that the photographic axes of both cameras are parallel to each other and at right angles to the base-line.

$$Y = \frac{b\,c'}{p_{x'}}\,; \qquad \begin{bmatrix} Z \\ X \end{bmatrix} = \frac{Y}{c'} \begin{bmatrix} z' \\ x' \end{bmatrix}.$$

The length of the base-line, employed in Darmstadt from 1962 through 1964, was $b = 1725$ m; the focal length of the stereo cameras is $c' = 101$ mm.

The picture coordinates, x', y', $p_{x'}$, are measured within the stereo comparator. While the accuracy of x' and y' is merely a question of proper identification of cloud points, the accuracy of the small value $p_{x'}$ is, as a rule, not great enough if $p_{x'}$ is measured only once. Due to the faint contrast of cloud points in the picture, $p_{x'}$ has to be determined by at least $n = 10$ independent measurements. Their mean, $p_{x'} = \sum^{n} p_{x'}/n$ is then of sufficient accuracy.

(II) An analogy to the $\Delta\alpha(|u|)$ — law represented by a thought experiment.

Despite quite different physical underlay, the statistical behaviour of a magnetic needle within a magnetic field is analogous to $\Delta\alpha(|u|)$.

It is defined that the magnetic needle

(1) is free to rotate around its center of gravity, if not exposed to a magnetic field (state of indifferent equilibrium; in motion, slightly "disturbed" only by friction); it also

(2) may be exposed to a homogeneous magnetic field of direction φ_0 and strength H; and

(3) due to friction, will come to rest pointing into a direction φ.

The deviation of the needles pointing direction from the field direction is defined as $\alpha_H = |\varphi - \varphi_0|$. Since the pointing of the needle with respect to the field direction is not ambigue by 180°, the range of variation of α_H is $\Delta\alpha_H \leq 180°$, instead of 90°. If the needle comes to rest after given a push, three quantitatively different stages, depending on $|H|$, can be distinguished (Fig. 12):

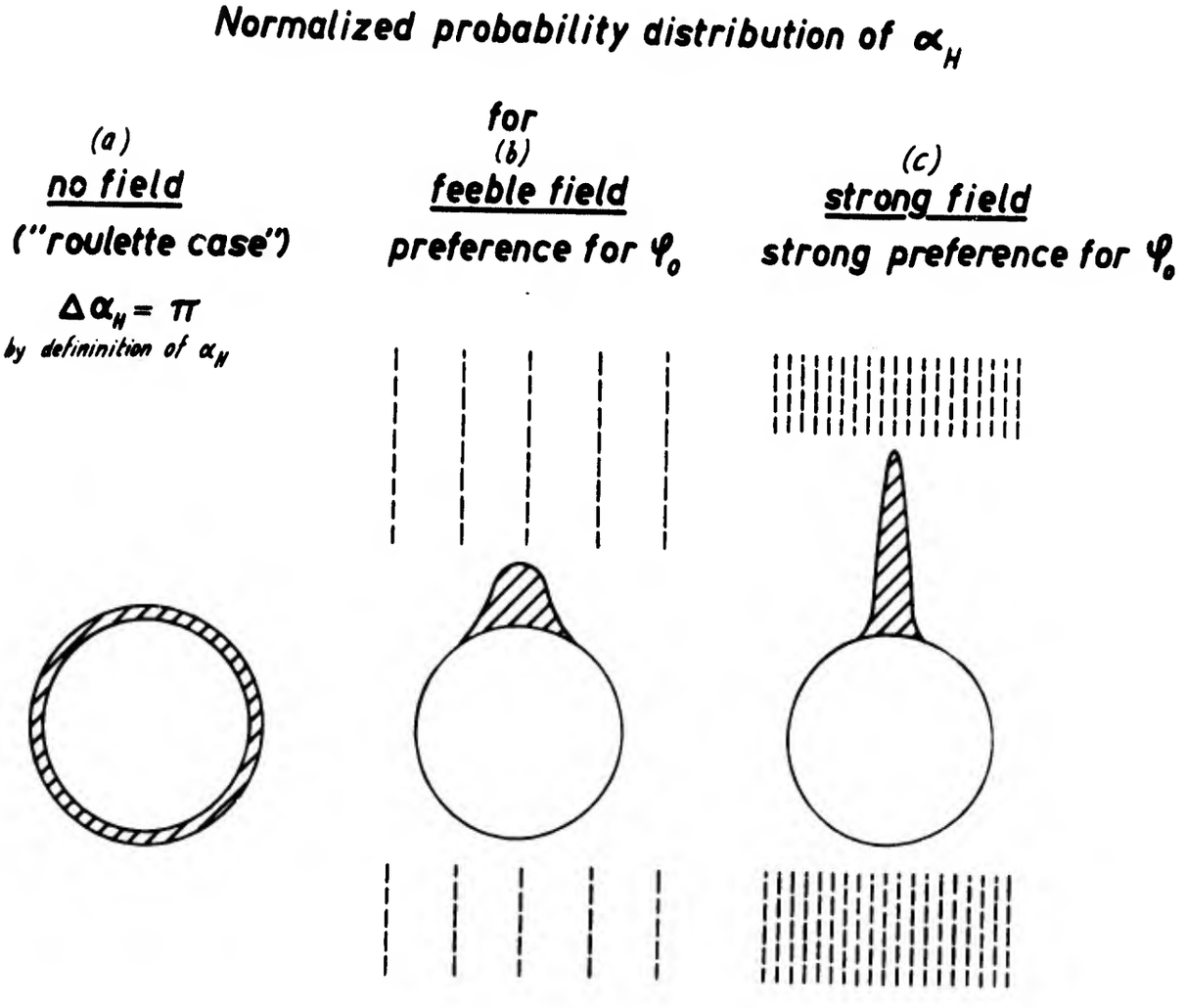

12 Illustration of the analogy of statistical behaviour

(a) At /H/ = 0, the needle may come to rest at any direction, all φ values being of equal probability ("roulette case");
(b) For small /H/>0, the needle, if pushed and coming to rest in many cases, will display a slight preference for the field direction;
(c) for great /H/, there will be strong statistical preference for the field direction.

Whether the frequency distribution of α is Gaussian, as suggested in Fig. 12, or if a distorted Maxwell function to both sides of that field line (which contains the center of the needle) exists, is a question of minor importance. At any rate the range of variation, $\Delta\alpha_H$, decreases toward increased field strength /H/. Therefore, in principle, $\Delta\alpha_H(|H|)$ behaves analogous to $\Delta\alpha(|u|)$.

(III) Determination of the $\overline{(\partial^2 u_r/\partial z^2)}$ value.

In a case of pronounced large scale ci-bands, the profile of the relative wind will be similar to that shown in Fig. 13 :
If we anticipate pronounced ci-bands to create at 300 mb, the layer approximately between 380 and 300 mb will have to be explored.
The wind hodogram (Fig. 13) demonstrates that the relative wind, from 380 mb on, has nearly the same direction through 300 mb, with an only slight, subsequent turn.
The dash-stippled line denotes both the position of the profile of the relative wind and the band orientation. For the resulting profile (Fig. 13 , lower left), those components of the 380 → 360 mb, ... ,.... 300 → 260 mb thermal winds are valid, which are oriented in the relative wind profile. (These components nearly equal the amounts of the thermal wind vectors, due to the small angular deviations from the mean direction).
The next step is to determine the mean $\partial^2 u_r/\partial z^2$ value of this

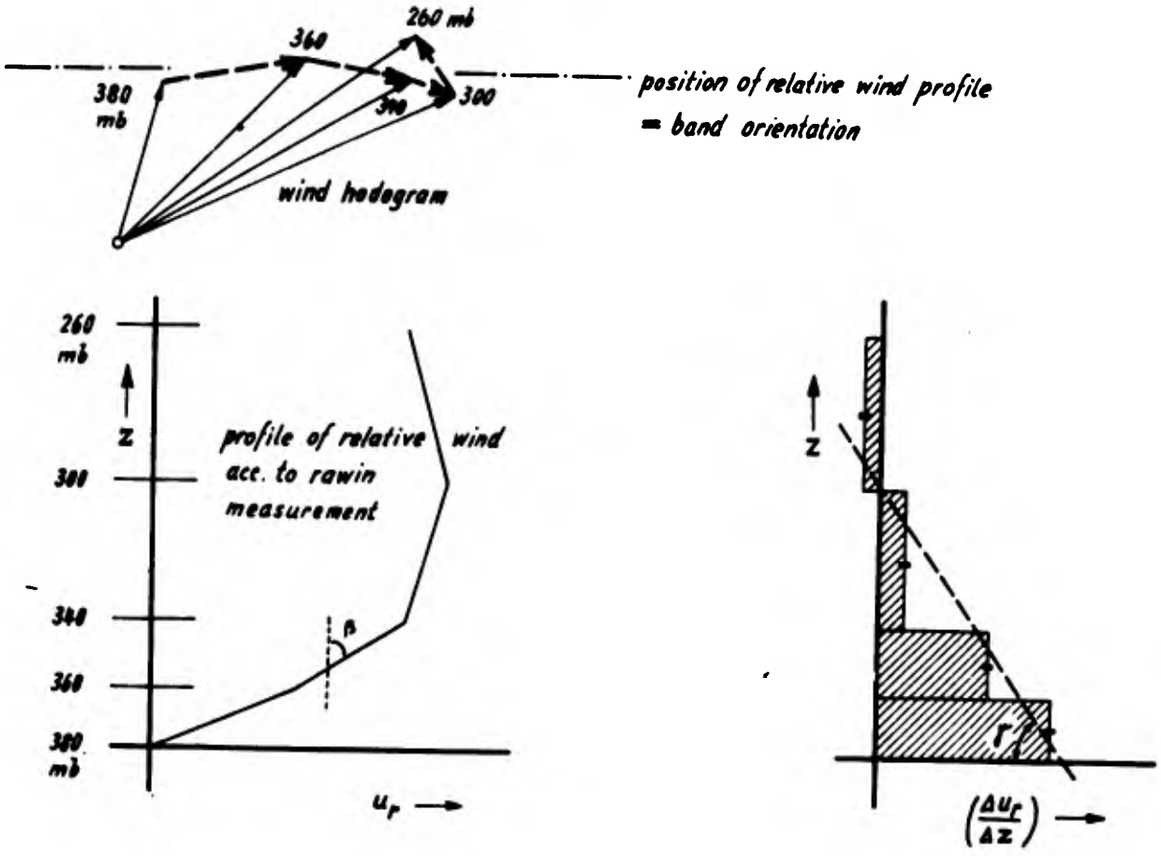

13 Scheme of method to derive the mean $\partial^2 u_r/\partial z^2$ gradient (KUETTNER value) from the actual wind hodogram.

actual relative wind profile, in order to find out whether it approximates the amount found by KUETTNER [11] for cu-streets. The method suggested is a semi-graphical one: Between two successive points of the profile, $\frac{\Delta u_r}{\Delta z} = \operatorname{tg}\beta$. In the right chart of Fig. 13, the corresponding $\operatorname{tg}\beta$ values - - four points in this case - - were marked. The slope $\operatorname{tg}\gamma$ of the equalizing line hence yields the vertical gradient:

$$\overline{\left(\frac{\partial^2 u_r}{\partial z^2}\right)} = \operatorname{tg}\gamma .$$

A second method consisted out of drawing parabolas of different parameters $p = \partial^2 u / \partial z^2$. Since, according to KUETTNER [11], $p = -1 \cdot 10^{-5} m^{-1}\ sec^{-1}$, parabolas were charted for $/p/ = 0.4, 0.6, \ldots 1.8, 2.0$, on foil. Superimposing these parabolas on the actual u_r profile by trial yields the p value which is closest to the actual value.

(IV) An account on the determination of vertical motions

by Dr. K. WEGE [1)]

The knowledge of vertical motion enables to draw conclusions on the stage which the observed cirrus clouds undergo. Therefore, the vertical velocities were determined for each of the cases, employing the methods advanced by PANOFSKY [16,17,18]. The total differential of the temperature of an air parcel reads

$$dT = \frac{\partial T}{\partial t}dt + \frac{\partial T}{\partial x}dx + \frac{\partial T}{\partial y}dy + \frac{\partial T}{\partial z}dz$$

which yields

$$\frac{dT}{dt} = \frac{\partial T}{\partial t} + v_h \nabla_h T + w \frac{\partial T}{\partial z} .$$

With the dry-adiabatic temperature gradient, $\Gamma = -\frac{dT}{dz}$, and the local vertical temperature gradient, $\gamma = -\frac{\partial T}{\partial z}$, the vertical velocity is

$$w = -\frac{\frac{\partial T}{\partial t} + v_h \nabla_h T}{\Gamma - \gamma} .$$

Thus w is obtained upon the local temperature change, the horizontal temperature advection, and the actual vertical temperature gradient. If the horizontal temperature gradient has a considerable component

---

1) Translation into English was made by J. REUSS

in the flow direction, while the local temperature change is $\frac{\partial T}{\partial t} = 0$, an air parcel proceeds along isentropes ($v \nabla \vartheta = 0$); if the temperature increases in wind direction, a subsidence is taking place - - and vice versa. For $v_h \nabla_h T = 0$ it is known that warming is caused by a general sinking motion, while cooling is caused by lift.

If advection compensates the local temperature change, the vertical component will be zero; on the other hand, the temperature may decrease despite warm advection (negative $v_h \nabla_h T$), whenever there is strong lift - - and vice versa.

Since, in general, the local change in temperature is known merely at 12 hour intervals, temperature advection must as well be determined for this interval. Hence only a 12 hour mean, taken along the length of the air parcel trajectory, can be obtained.(Therefore, in the table which summarizes parameters of the six cases of this report, the vertical velocity derived by the above formula, was denoted w_{12}. In a few cases where 6-hour-interval observations were available, it was also possible to calculate w_6).

This method, in some altered way, was also employed for research on cirrus clouds, by LUDLAM and MILLER [13] . However, these authors partly did not take the local temperature change in consideration.

The above method still bears some disadvantages and inaccuracies which shall be discussed briefly in the following.

In the interest of a time-saving procedure, geostrophic conditions were anticipated and no trajectories determined; non-adiabatic processes were not considered: Moist-adiabatic and sublimation-adiabatic lift, which is likely to have existed in the present cirrus cases. The deviation of both from the dry-adiabatic temperature gradient is in the order of $0.1 \div 0.2 \left[°C/100\ m\right]$ in the upper troposphere.

Another disadvantage is that the relative error in the amount w becomes great if γ approaches the value of Γ . -

Radiation represents a non-adiabatic process also not considered in our calculations; at ci-levels, it causes a daily amplitude of 0.5°C, which is responsible for a, merely apparent, additional subsidence from 00 to 12 hours, and apparent ascent from 12 to 24 hours, both superimposed on the determined vertical velocities.

The error which is caused by determining $\left(\frac{\partial T}{\partial t}\right)_{12}$ not for a constant altitude but for a level of constant pressure instead, can be neglected in advance since the geopotential change is in the order of a few geopotential decameters, in our cases.
Errors in radiosonde measurement may, of course, induce considerable falsifications of the vertical motions; for this reason, attention was paid to the question whether the radiosonde measurement results were reliable.
Summarizing all these possible errors, an uncertainty results in the amounts but hardly in the signs of vertical motion.-Local advection, as is known, is determined upon the wind change with height, by

$$\nabla_h T = \overline{T}\,\frac{f}{g}\,\frac{\partial \mathbf{v}_h}{\partial z} \otimes \mathbf{K}.$$

In this relation, $\otimes$ means vector multiplication; $\overline{T}$ denotes the temperature mean of a layer of thickness ∂z; f is the coriolis parameter; g means the gravity accelleration and $\mathbf{K}$ denotes the vertical unity vector. Multiplying this equation by $\mathbf{v}_h$, yields the advection at the left side of the equ., while the right side contains the term $\mathbf{v}_h(\partial \mathbf{v}_h \otimes \mathbf{K})$. $(\partial \mathbf{v}_h \otimes \mathbf{K})$ denotes a vector within the plane of the paper, since $\mathbf{K}$ is perpendicular on the paper plane; it is also at right angle with respect to $\partial \mathbf{v}_h$, and has an angle β with respect to $\mathbf{v}_h$; its amount is $|\partial \mathbf{v}_h|$ (see Fig. 14).
The scalar product of $\partial \mathbf{v}_h \otimes \mathbf{K}$ and $\mathbf{v}_h$ is $|\mathbf{v}_h| \times |\partial \mathbf{v}_h| \times \cos\beta$, accordingly, which is equal to twice the area of the triangle of Fig. , since $H = |\partial \mathbf{v}_h| \times \sin(90-\beta) = |\partial \mathbf{v}_h| \cos\beta$.
Since also $H = |\mathbf{v}_h + \partial \mathbf{v}_h| \times \sin\alpha$ exists, the local horizontal temperature advection is expressed by

$$\mathbf{v}_h \nabla_h T = -\left(\frac{\partial T}{\partial t}\right)_{adv} = \frac{f\overline{T}}{g} \times \frac{|\mathbf{v}_h| \times |\partial \mathbf{v}_h| \times \cos\beta}{\partial z}$$

$$= \frac{f\overline{T}}{g} \times \frac{|\mathbf{v}_h| \times |\mathbf{v}_h + \partial \mathbf{v}_h| \times \sin\alpha}{\partial z}$$

The advection at ci-level was determined with the right term. Following a proposal made by CONOVER, a layer of thickness $dz \hat{=} 100\ mb$ was used, in the middle of which cirrus would occur. The negative sign of the left term results since a positive value of $\mathbf{v}_h \nabla_h T$ means cold advection.
A second method was employed to determine the vertical velocity, then called w_{adv}.

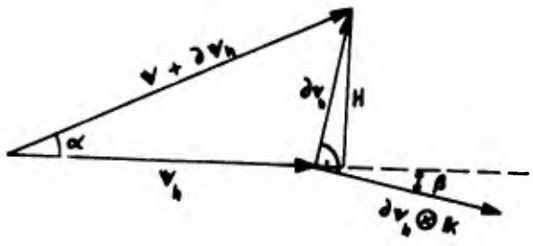

14 : vector arrangement (see text).

This method consists in substituting the horizontal temperature advection which results from the wind profile (by the above formula), for the horizontal temperature advection which results from the horizontal wind and temperature distribution. This method bears the disadvantage that the 12 hour local change in temperature is linked with an instantaneous - - and hence inaccurate - - value of advection. Moreover, the wind values are of sufficient accuracy only for greater α, since for small α, $\left(\frac{\partial T}{\partial t}\right)_{adv}$ is greatly influenced by changes of wind direction as small as 10°. Despite this, w_{adv} was included, for comparison, in the table under the subsequent paragraph.

(V) Theory of relations between vorticity advection, vertical motion and cirrus cloud occurence, according to [9].

J.E. FRENCH and K.J. JOHANNESSEN [9] advanced a method of forecasting wide-spread cirrus clouds by means of high-level contour patterns: For the generation of extensive cirrus clouds, large scale ascent is necessary. The vertical motion field can be derived by the equation of continuity and the vorticity equation. From these two, we obtain, with disregard to e.g. the change of the Coriolis parameter along the contours, the following relationship:

$$\frac{dp}{dt} = \frac{(u-c)(p-p_o)}{\psi + f} \cdot \frac{\partial \psi}{\partial s} \quad ,$$

where $\frac{dp}{dt}$ (the individual pressure change) is the vertical motion in the p - system, ψ the relative vorticity, f the Coriolis parameter, u the wind velocity, c the speed of a vorticity line along the contour s, p the pressure level in question, and p_o a pressure level which is assumed to be the zero-level $\left(\frac{dp}{dt} = 0\right)$.

In most cases $c < u$ (usually $c \approx \frac{1}{2} u$).

French and Johannessen assumed the tropopause as the level of no vertical motion. This equation shows the well known relation between

vorticity advection and divergence. Positive vorticity advection ($\frac{\partial \psi}{\partial s} < 0$!) is combined with divergence; as the maximum of divergence is at the zero-level (near the tropopause), we have ascending motion at high levels below the tropopause and subsidence above, and vice versa.

In order to compare this theory with our cirrus observations and our computations of the vertical velocity (see preceeding chapt.), the distribution of the relative vorticity for a contour pattern near the cirrus clouds is given for each case. In connection with this contour pattern we obtain $\frac{\partial \psi}{\partial s}$. As all cirrus clouds were observed in the troposphere, the sign of $\frac{\partial \psi}{\partial s}$ shows whether the theory is in agreement with the observations.- The (geostrophic) relative vorticity was computed with a four point formula:

$$\psi_g = \frac{g}{f h^2} \; (z_1 + z_2 + z_3 + z_4 - 4 z_o) \; ,$$

where z_i are the geopotentials, h the mesh-width (h = 300 km was chosen), and g the gravity acceleration.

Like in one case encountered by the authors [9] , this theory did not clearly apply to our cases which - - with merely one exception (case III) - -- occurred close to a High ridge. Perhaps the applicability is in general confined to situations -- and to the extent -- in which wind is very slow or in which its direction is nearly the same throughout the troposphere.

case study I: 13 May 1963

1. Introduction.

Beside case IV, this case represents one of the rarely encountered in which the orientation of pronounced large scale ci-bands deviates considerably from the wind direction of their level. Moreover, the present case is pronounced to such degree as to reveal the independent existence of what will be explained and defined as a "thermal jet stream" (see paragraph 2.1.2.).

Cirrus bands which extended from the northern to southern horizon were observed in Darmstadt from 7:00 till 16:00; (for details, see Table I).

Single camera photographs were taken from 7:15 through 15:16, with stereo photography from 10:54 through 12:25. The main results of photogrammetric measurements were summarized in Table I; for an improved survey on stereo data, the period of stereo photography was subdivided into 4 time intervals.

These data should guide through the details reported and meteorological conclusions drawn in the current text.

2. Bands' properties and meteorological environment.

2.1. Large scale. Over the Darmstadt area, pronounced ci-bands at an altitude of 7.0 km and of lengths exeeding 300 km occurred at least from 7:00 through 16:00 (Figs. 4,10,11,16,17). Their orientation was, throughout, $0^{\circ}\leftrightarrow 180^{\circ}$, with deviations of only $\pm 5^{\circ}$. These small variations in orientation were not steady nor systematic, but apparently "incidental" as to both time and position -- depending on the respective momentary and local wind condition.

Large scale band spacing, i.e. transversal distance of band axes, was in the order of magnitude of 10 km throughout. This band system travelled with the motion vector changing from 335°, 13 m/sec at 8:15 over 296°, 7m/sec at 11:50, to 251°, 11 m/sec at 15:10 (compare Table on next page).

Properties of banded and non-banded ci over Darmstadt on 13 May 1963, 7:15 till 15:00.

ci depicted in Fig.	time [Z]	altitude [km]	motion vector: move from	motion vector: vel. [m/sec]	band orientation	streak orientation	remarks
1	7:15		NW		3°↔183°	streaks did not exist yet	
2	8:15		335°5	13.4	5°↔185°	97°→277°	
3	8:45		--	--	--		
4	8:30		327°	13.4	--		
5	9:00	7.2*)	not meas.	13.0	1°5↔181°5	113°→293°	
-	9:10		317°		3°↔183°±3	not pronounced	
6b	9:30		318°	not meas.			
7a,b	10:00	≈10.7	316°	9.2	112°↔292°		band spacing 0.2 km; moderate convection, small scale lateral motion.
		(base:					
8	11:00	10.65	311°	11.8	117°↔297°		
	11:28	6.65	not exactly measurable 1)	--	--	115°→295°	--
	11:42)	7.0	296°	6.7	4°↔184° over Darmstadt 178°↔358° west of -"-		marked ci-band
9,10,11,12	11:30	9.5	311°	8.4	--		small single cloud
like in 9	11:45	6.9	296°	6.7	4°↔184°		
13	11:55	8.8	284°	9.4	0°↔180°	single, narrow ci-band	
--	11:50	10.2	295°	11.3	--	single small cloud	
	12:15	6.9	275°	6.8	176°↔356°	first ci-band with strong convective activity	
	12:25						
14	12:20	10.5	278°	12.6	--	thin sheet	
		11.4	282°	8.7	3°↔183°	thin, dappled sheet	
15,16	13:40	7.0*)	≈263°	not meas.	174°↔354°		
17	15:10	7.0*)	251°	11	176°↔356°		ci-bands of rugged appearance. ac lent
		3.2*)	210°	4.5	--		

stereo measurement

*) according to estimates of the Bismarck-Turm weather station, near Darmstadt

1) motion vector did not deviate much from that of ci-bands at 7.0 km.

Graphical representation of cirrus motion vectors (altitudes in circles); [from Table on p. 42]

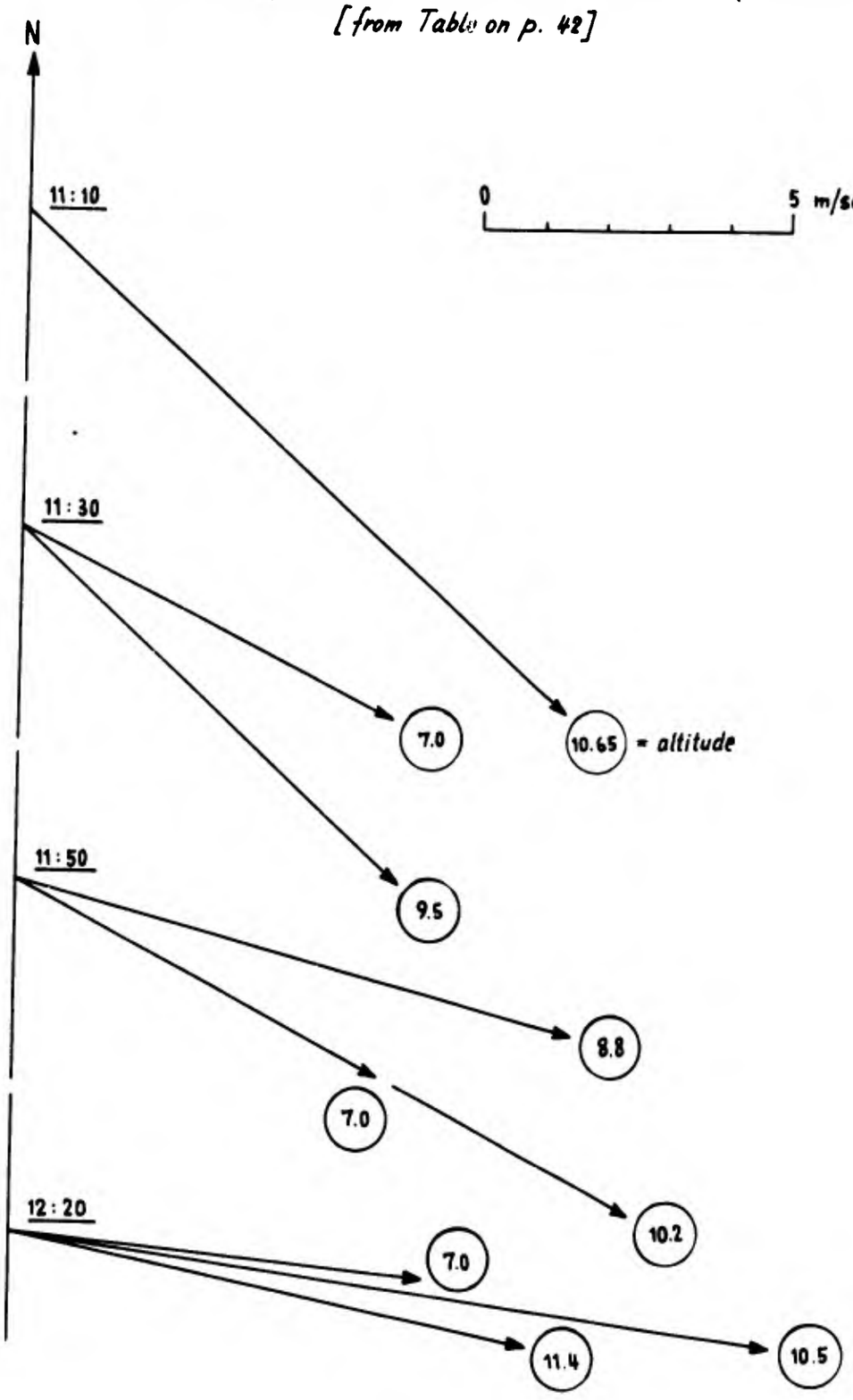

The ci-bands approximately paralleled isotherms, isonephs, and isohumids (Figs. 24,25,35,36,38), the mean isoneph amount decreasing with increasing mean difference between dew point and dry temperature. The amount of cloud cover which -- especially in its eastern portion -- mainly consists out of ci-bands, steadily decreases from W forward E, becoming zero -- at least at ci-level -- close to the "thermal jet stream" (the latter is defined in the subsequent paragraph).

2.1.2. Wind properties over Germany at 12:00 can be overlooked best in Fig. 29; it shows that, roughly along the line Wernigerode → Stuttgart (St), a maximum of vertical wind shear occurs between 500→400 mb, which lay slightly east of Darmstadt (Da). Some 130 km eastward, roughly along the line Berlin (B)→Munich (MU), the vertical wind shear maximum is between 400→300 mb. It is hence plausible that, roughly along the line Hannover (Ha)→Wiesbaden (Wi), but with reduced amount, the maximum of vertical wind shear has shifted down to -- approximately -- the 600→500 mb shearing layer (concluding from the relative wind hodograms of Hannover and Idar-Oberstein).

With regard to Figs. 24,25,26,27,29,30,35,36,38 this suggests the following conclusions as to the aerological state: A "layer" occupied by the maximum horizontal temperature gradient rises from west to east (Fig. 15): It apparently represents a softened high level warm front[1] (compare Fig. 30) which separates the western high level warm "sector" (Figs. 24,25,30) from the eastern moderately warm air mass. It is obvious that this layer of maximum horizontal temperature gradient is also a layer of maximum vertical wind shear which -- disregarding of ageostrophic effects -- is directed along the isotherms; we therefore call it the "thermal jet stream" (thJS). At 12:00, the maximum of vertical shear is estimatedly at 340 mb over Berlin→Munich, and at 460 mb over Wernigerode→Stuttgart. Concluding from the vertical wind shear measured at 06:00 (Fig. 28), its maximum at 06:00 was between 280 ÷ 320 mb over Berlin→Munich, and roughly at 430 mb over Wernigerode→Stuttgart. This

---

[1] It may be compared to what KUETTNER [11] called a jet front, with the difference that the latter, in most cases, represents a cold front.

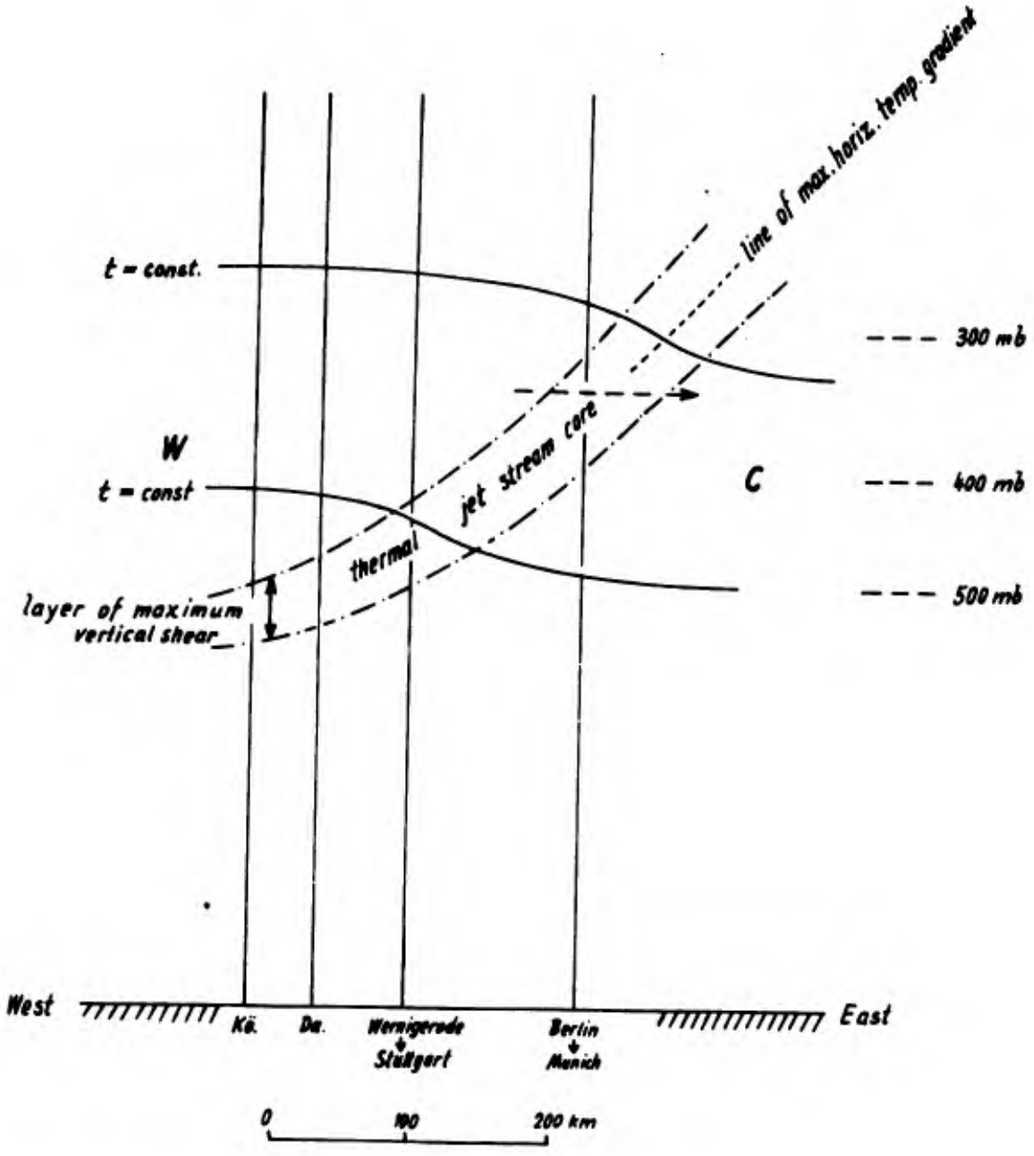

15 : Semi-quantitative scheme of vertical cross section through thermal jet stream at 12:00, of 13 May 1963; at 06:00, the thermal jet stream core was approximately 100 km west of - - and correspondingly higher than - - the 12:00 position. Compare Figs. 28, 29, 30, and current text.

local decrease in altitude with time reflects the slow west→east migration of the system (see arrow in Fig. 15), accompanied by a west→east shift of the isonephs (Fig. 38).

East of Darmstadt, the thJS produces a backing of the wind direction with height by nearly 180°, since the thJS is directed nearly opposite to the winds below it.

Over Darmstadt at 12:00, according to Fig. 39, the strongest shear must have been close to 500 mb or even a little lower; this explains why stereo measurements of motion vectors of fall streak fragments as low as 440 mb did not disclose strong wind shear.

The thJS obviously is nearly independent of the great changes in the direction of the winds, which e.g. changes for 85° within 7 hours at 400 mb (over Darmstadt), with the eastward component dominating (Table I, and paragr. 3, and comparison of Figs. 28,29).

In the following, in accordance with chapt. 2.2., we define as "relative wind" u_r the (relative) wind vector -- at any altitude exceeding the 500 mb-level -- which one obtains if the 500 mb wind vector is subtracted; (the relative wind of 500 mb is hence equal to zero).

The KUETTNER profile of the relative wind, at Stuttgart taken in the vertical plane oriented north↔south, i.e. which contains the line of strongest vertical wind shear (500 mb→455→430→420→400 mb, see Fig. 29), yields the mean value $(\partial^2 u_r/\partial z^2) \approx -1 \times 10^{-5} [m^{-1} \text{ sec}^{-1}]$ for Stuttgart at 12:00, in the layer approximately between 500 and 350 mb. This is equal to the amount predicted by KUETTNER but originally conceived for relative winds which parallel the general flow direction. Over Darmstadt, also at 12:00, the altitude of this profile was apparently -- in accordance with the scheme explained above (Fig. 15) -- some 0.7 km lower than over Stuttgart. The ci-band level thus marks the altitude at which vertical shear has ceased considerably. The pronounced character and largely uniform behaviour of the thJS shearing layer -- uniform as compared to the variation of actual wind direction, has justified to discuss and define it in advance of the description of high level weather (paragraph 2.1.4.).

2.1.3. Surface weather development:[1] At 06:00, a stationary blocking High extends over European Russia; its western part, separated by an almost stationary front, extends to the Oder river area (Fig. 18). It is diminished rapidly and pushed eastward by a severe storm Low, the center of which is located 400 km south of Iceland. Also at 06 hours the frontal system of this Low permits a -- then already narrow -- warm sector to extend from the North Sea (east of Britain) through northern France. (As the cross section demonstrates [Fig. 30], a second warm front exists at higher levels which does not reach the surface but is most important to the generation of the cirrus here discussed).

In the course of the forenoon, the warm front becomes occluded. The now slowly proceeding cold front crosses Darmstadt around 17 hours; at midnight, it has reached the line Milan-Munich-Danzig (Fig. 18, dashed line). This course is reflected in the surface pressure change: At 06, 09, 12, 15, 18, 21, and 24 hours, the sea level pressure [mb] at Darmstadt was 1021.4, 19.0, 16.0, 13.8, 14.5, 16.6, and 1018.8, respectively. Minimum pressure, with 1013.0 mb, occurred at 16:40, followed by an immediate increase by 0.2 mb and of another 1.3 mb in the course of the subsequent hour. Light drizzling rain set in at 17:20, after passage of the cold front; a first measurable amount of 0.3 mm was recorded at 18:00, with very slow rise until 19:00, the increase becoming a little steeper until 21:40, when a total of 4.6 mm was recorded. There was no more rain in Darmstadt at least until 7:00 of the next day.

The cirrus bands observed over Darmstadt in the forenoon may have occupied the moderate warm air which lies east of the high level warm front and still above the eastern warm front. Their isonephs were of small amount, decreasing toward zero approx. 100 km east of Darmstadt (Fig.38, 9:00); their convective activity was very feeble.

By far the greatest amount of cloud cover occurred at noon and afternoon, which at this time were in the high level warm "sector"; they displayed strong convection activity.

2.1.4. Development of high level synoptic situation:[1] At 13 May 63,

[1] According to the synoptic analysis and comments made by Dr.K.WEGE.

0:00, a smooth through extends south north some 300 km east of Darmstadt, both in the 500 and 300 mb levels. In front of the high-reaching Low in the northeastern Atlantic, a High ridge extends from Spain over France up to southern Norway. Its eastern part induces a wind from north over West Germany. As a consequence of the changes described in the foregone chapter, this High ridge moves southeastward, thereby weakening over Germany. This slow motion of the High ridge is well reflected in the subsequent wind and cloud motion directions (see Fig. 28a,b, and Table on p. 42 of this volume).

For instance, the 300 mb-wind over Köln (10 513) changes from 350° at 00 over 310° at 06 to 220° at 12 hours, "ending" with 180° at 18 hours, thereby weakening toward 18 hours and becoming stronger again from this time on. Likewise, the Köln 400 mb-wind blows from 350° at 00, followed by nearly calm air at 06 and slow winds from 220° and 190° at 12 and 18 hours, respectively. Similar behaviour can be noted with the winds at Idar-Oberstein (Fig.). In our Table, ci-bands at 7.0 km over Darmstadt moving with an average of 10 m/sec change motion directions from 335° at 8:15, over 296° at 11:45, to 251° at 15:10.

The most rapid change in motion direction over Darmstadt, from 296° to 275°, takes place from 11:45 to 12:20 at 7.0 km (see Table). Accordingly the High ridge axis in the 400 and 300 mb contour pattern lies approximately over Darmstadt.

The greatest horizontal temperature differences occur along the cold front (Fig. 30, left); it has the steepest slope to the effect that the areas of strongest horizontal temperature gradient at different levels are relatively close together.

These conditions generate an 80 knot jet stream which is linked with a "break" in the tropopause (Fig. 30, outer left), while over Darmstadt comparatively weak pressure gradients prevail. This jet is part of the strong winds over the Atlantic. Another jet branches off southward into the western Mediterranean (Figs. 22,23). This generates a zone of extreme diffluence with its center some 200 km southwest of Darmstadt, accompanied by divergence -- as the pressure decrease at the surface suggests.

The pattern of diffluence of the 400 mb thermal wind lies still farther to the southwest of Darmstadt as suggested by a comparison of Figs. 22,24,26,27.

While over Germany the thJS is embedded in a zone of slow winds, it

joins the jet stream headed toward south: The 400/500 mb thJS flows into the 400 mb jet stream, while the 300/400 mb thJS joins the 300 mb jet stream -- and becomes part of the latter -- over the northwestern Mediterranean (Figs. 22,23).

2.1.5. Advection, temperature changes and large scale vertical motion. Temperature advection over the area of Darmstadt, on 13 May 1963, in the 350/450 mb layer as computed by the sounding of Idar-Oberstein (100 km west of Darmstadt), was
in the forenoon:

$$\left(\frac{\partial T}{\partial t}\right)_{adv} = 0.32 \times 10^{-5}\ [^{\circ}C \times sec^{-1}] = 0.14^{\circ}/12\ hours;$$

in the afternoon:

$$\left(\frac{\partial T}{\partial t}\right)_{adv} = 1.9 \times 10^{-5}\ [^{\circ}C \times sec^{-1}] = 0.82^{\circ}/12\ hours;$$

(in here, t denotes the time!).

Slow ascent of air, as calculated for Köln (Kö) by the formula of PANOFSKY [18], under the assumption of geostrophic conditions, was as follows:

(1) In the mean over 0:00 till 12:00: at 500 mb, w_{12} = +1.9 cm/sec,
at 300 mb, w_{12} = +2.2 cm/sec;
(2) in the mean over 12:00 till 24:00: at 400 mb, w_{12} = +2.3 cm/sec,
at 300 mb, w_{12} = +1.3 cm/sec.

If in the formula for the ascent velocity, $v\nabla T$ is substituted by $-\left(\frac{\partial T}{\partial t}\right)_{adv}$, its amount being derived by the actual vertical shear vector [see Appendix, paragraph (V)], the ascent velocity in the 400 mb level over Idar-Oberstein results:

In the forenoon : w_{adv} = +2.5 cm/sec;
in the afternoon: w_{adv} = +2.4 cm/sec.

These amounts suggest that the ascent velocity had a soft maximum close to the 400 mb level. Hence these cirrus were generated by large scale ascending motion which could be expected to occur in front of, and above, the frontal system of the extensive cyclone south of Iceland. In coherence with the observed decrease in surface pressure, we may assume that an area of divergence existed with its vertical maximum between the level of the lower ci (≈7.0 km) and the tropo-

pause. For more detail about temperature changes, lapse rates, humidity etc. see the summarizing Table.

2.1.6. Humidity at 12:00 had a maximum -- with mean amounts of 80 % between 530 and 430 mb, both in Idar-Oberstein and Köln (Figs. 31, 32). This layer is only little higher than the layer of strongest vertical shear at these stations (500/600 mb thJS, Fig. 29).

The humidity values measured over Stuttgart are apparently wrong, since despite the cirrostratus observed there, the measured humidity did not increase at or below ci level.

Saturation with respect to ice existed both in Idar-Oberstein and Köln.

2.1.7. Vorticity advection. At 12:00, the ci-bands were situated in an area of negative vorticity advection (Figs. 21,23,39). Hence the present case does not comply with the theory of FRENCH and JOHANNESSEN [9], especially since the PANOFSKY formulae [16,17,18] yield large scale ascent and the bands display moderate to strong convective activity.

However, positive vorticity advection sets in at a point about 300 km upstream of Darmstadt (Figs. 21,22,23,39).

2.2. Small scale.

In the early morning of 13 May, ci-bands appeared comparatively faint (Figs. 1,2) with little convective activity and rather little small-scale motion. This enabled to identify a cloud point through an interval of half an hour (Figs. 3,4). Convection increased toward moderate in the course of the forenoon; at this time, bands were not yet pronounced to the degree of those seen in the early afternoon (Figs. 15,16). With increasing band density fall streaks also increased; they pointed toward 277° at 8:15, changing toward directions between 285° and 295° at 11:30 (Fig. 9).

Stereo viewing and evaluation of pairs taken at 11:30 demonstrates this: In their upper portion, particles fall from band base towards the observer; then, some 250 m below the band base they sharply

bend toward west, apparently in a very shallow layer of strong shear. (This layer is by far too shallow as to affect large scale banding. The large scale shear which generates bands is still below this shallow layer).

At 9:45, a layer of narrow bands with an average widths of some 2.2 km -- equal, in this case, to their spacing -- occurred and prevailed until 11:20, within this time no other bands occurred. The last stereo photograph of this layer of narrow bands was taken at 11:10; the last single photo showing them is at the upper portion of Fig. 10, (11:15), marked by a dashed arrow at outer left. These narrow bands showed considerable lateral motion: While a point at the NE side of a band (in Fig. 7) moved from 314°, a point at its SW side moved from 318° (Fig. 7c); this implies a lateral motion of 0.24 m/sec each towards both sides of the axis; roughly one hour later, (Fig. 7), the lateral motion had increased to 0.30 m/sec. More precise and detailed measurements were not possible since the cloud spots quickly loose identity. Orientations of these narrow bands were 117°→297° at 10:00, 110°→290 at 11:00, in fair agreement with the 260→235 mb vertical shear at Stuttgart (Fig. 29). Bands which occurred 7.0 km over Darmstadt at 12:20 displayed strong convective activity to the effect that most of the cloud features loose their identity within three minutes (Fig. 14); whereas higher ci, at 10.5 and 11.4 km, showed no changes in their pattern.

Band spacing comes close to regular in Fig. 15b: Five different bands can be distinguished with spacing (from E to W) 6.3, 9.0, 6.4, and 7.3 km. (Two of these bands were omitted in the map of Fig. 16; see identity numbers in photos and map. Apparent greater spacing in the map, east of Darmstadt may be due to a foreshortening effect by which spaces between bands may have been omitted).

From the pronounced band in the foreground of Fig. 15a, dense fall streaks fell into the layer of strongest shear -- which determines the band orientation -- so that this band's lower portion looks nearly straight.

As the details of bands suggest, stronger convective activity set in again toward 15:00 (Fig. 17). This time, clouds which resemble ac lent were also present, the shape of which also changed quickly to

the effect that they, also, lost identity within minutes.

It may have been noted that characteristic cloud features, and the rate of change of identity, prevail along the band throughout great lengths -- if not even the entire lengths -- of the bands. It were these empirical facts which first suggested the assumption that rather pronounced, large scale bands also parallel isopleths of stability criteria (compare pages 16a, 17, 18).

3. Discussion of results.

3.1. In view of the small travel velocity of these ci-bands, the great range of deviations of their large (and small) scale orientation from their motion directions, is permitted by the $\Delta\alpha'(|u|)$ statistical law.

3.2. This case also corroborates earlier observations (e.g. REUSS [20], see summary there) which imply that α of such great amount and for pronounced ci-bands in most of the cases are associated with bands located close to a High ridge.

(In this connection the following appears worth to be mentioned: In a TIROS IV photograph taken at 16:30 on 11 Febr. 1962, of an area near 37°N, 40°W, BUSCHNER [2] recently found a vortex which opposed to common expectations was not associated with a Low, but to a cold air "drop" in the 500/1000 mb relative topography (this expression being used for "thickness pattern"). According to the figures which represent the synoptic situation, this vortex -- hence with cloud bands which also deviate considerably from the contour [or wind] pattern -- also occurred in a typical High ridge present at all levels from surface up to 500 mb).

3.3. Vertical wind shear, both large scale and strong (15×10^{-3} sec^{-1}), was necessary to generate bands which prevailed for at least 10 hours, in great horizontal extent and in nearly straight lines. There can be no doubt that the bands at about 420 mb were produced by and oriented parallel with the great 600→400 mb mean vertical shear (Figs. 28, 29). Correspondingly, all of the ci-bands near Darmstadt paralleled the 400 mb isotherms (Fig. 24) and the 400/500 mb relative topography (Fig. 26). This still holds true for the 300 mb-isotherms and the 300/400 mb relative topography (Figs. 25,27).

The large scale profile of the relative wind 500→350 mb, as to be deduced from the Stuttgart winds in Figs. 28, 29, is in fair accordance with the shear gradient value postulated by KUETTNER [11].

3.4. The bands of Figs. 15,16 bear resemblance to bands measured by CONOVER, in [6], Figs. 121-123; the main difference is merely this: While in case No. 10 of [6] the shear within the layer of maximum shear (thJS) was nearly parallel with the wind (of great velocity) at its level, the shear within the thJS, in the present case, was at great angle with respect to the wind (of small velocity).

3.5. The horizontal and vertical maximum of large scale vertical wind shear has been denoted as a "thermal jet stream" (thJS). It follows from this definition that the vertical cross section area occupied by the thJS is identical with that of the frontal layer, i.e. the sloped layer of increased horizontal temperature gradient (called jet stream front in "normal" JS by KUETTNER [11]). Unlike surface conditions, the high level "front" is associated with a relatively smooth and steady temperature change (in a level of constant pressure), as compared to a front near the surface. The thermal jet stream core (or axis) -- in the line of strongest shear and maximum temperature gradient (in p = const level) -- therefore, has different positions at different levels (Figs. 28,29,30).

3.6. Bands in the moderate warm air -- over Darmstadt in the forenoon -- showed only small convective activity; while bands in the high level warmest air displayed (1) quick changes in their small scale patterns, which led to (2) a rugged appearance (Fig. 17) and (3) local changes of the apparent condensation level (some hundred meters on distances of a few km).

3.7. Within the narrow bands at 10.6 km which occurred at 10:00 until 11:00 and within the warmest air, small scale lateral motions were found which confirmed earlier findings of CONOVER [6,7], as to both kind and mean velocity of these motions.

3.8. A case rather similar to this one as to both cloud and meteorol

ogical aspects was encountered on 24 May 1964[1]: All the day long, strong shear 500→400 mb prevailed near Darmstadt, causing band generation close to 400 mb. The shear maxima were arranged within a high level warm front similar to that represented by Figs. 28, 29,30.

3.9. On the small scale, finally, a ratio (spacing/ thickness of shearing layer) of roughly 3 prevailed at both the large scale (Figs. 10, 15, 16) and narrow bands (Figs. 7, 8): At the large bands, mean spacing was some 7 km, with a shearing layer of some 2.4 km thickness (from lower boundary of strongest shear, up to band tops). At the narrow bands, spacing was some 2.2 km, with a shearing layer of some 0.7 km (Stuttgart, 260 → 235 mb).

---

1) This was a Sunday; this permitted only to take single photos; cirrus altitude was determined as average of estimates of several meteorological stations including the Rhein-Main-airport.

case study II: 2 March 1957

1. Introduction.

The cirrus bands herein described were taken by predecessors of the author, Messrs. H.G.NEUMANN and H.SCHULZ. The photogrammetric base was 1.790 m in length, oriented $167^g \rightarrow 347^o$, and located some 6 km west of Darmstadt.

The diary records "some pretty ci at 7 hours; at 8, ci uncinus at North; at 9, very long (extended), cross-striped ci, yet too faint for photography. Good visibility, no fog ..... At 9:30, less ci in zenit, but increased ci-cover in northwest. At 10:30, faintly visible ci merely near the horizon; clear sky in zenit; jet plane condensation trails diminish within seconds. At 11:00, still cloudless in zenit, faint ci near horizon. At 11:30, ci were seen approaching from North."

From 11:43 on, photographs were taken first by the southern camera at 11:43, 11:48, 11:50, and 11:55 (Fig. 1). Stereo photographs (Figs. 4,6) were taken toward zenit at one-minute intervals, from 12:06 until 12:28, followed again by some single camera photographs until 13:00. These photographs and further observations till 13:30 showed that a tendency towards random masses of thin ci-sheets prevailed in the "wake" of the rather pronounced ci-bands.

To the extent to which it could be explored, this ci-band case closely resembles the general scheme advanced by CONOVER ([6], type Ib) -- compare Figs. 2,9,16 -- but with no front reaching down to the surface.

2. Bands' properties and meteorological conditions.

2.1. Large scale:

During the period of measurement, the average altitude of band level was 10.1 km; a few fall streak ends were as low as 9.5 km. The motion of the band system was 4^o,34 m/sec. The orientation of the band depicted in Figs. 1,3 was about $10^g \rightarrow 190^o$ in the foreground (down to point (2)); behind point (2) it changes to about $0^g \rightarrow 180^o$. Concluding from the diary notes and Figs. 1,3 the band of which a portion is depicted in center of Figs. 1,3 must have had a length of at least 150 km. The spacing of a total of four bands, as derived by rectification of Fig. 7, was -- from east to west -- 14, 8, 6 km. A curvature

of the band axes, as recogniseable in Fig. 7, is concave toward east, its mean radius being some 200 km. On the whole, the ci-bands parallel both isotherms (Figs. 10,11,12) and isonephs (Fig. 2) close to their level. Also the isohumids (Fig. 14), which could be obtained completely only for the 400 mb level, are in plausible agreement with the isonephs.

2.1.1. Wind conditions can best be overlooked by Fig. 13: At 15:00, all 250 mb (= ci level) winds at Bitburg (Bi), Hannover (Ha; 225 mb), Wiesbaden (Wi), Stuttgart (St), and Munich (MÜ; 285 mb) blow from 0° = north, uniformly, according to the respective rawin measurements. The arithmetic mean of the wind amounts at Wiesbaden and Stuttgart at 14:00 is 33 m/sec.

These values agree well with the motion vector of ci-bands as measured at 13 hours in Darmstadt: 4°, 34 m/sec. The mean vertical shear vector 300→250 mb, also at 14:00 is 325°, 7×10^{-3} sec^{-1}. Thus, its direction roughly agrees with the pointing of the fall streaks which occupy the layer from 9.9 down to 9.5 km (Figs. 3,4, and lower left of Fig. 5a).

For the wind conditions under which the ci-bands were born the ascent of Stuttgart, located in the lee of Darmstadt, appears to be the most representative. If we substitute 4° as the 250 mb wind direction, a mean shear vector 300→250 mb = 350°, 9.7×10^{-3} sec^{-1}, results. The mean shear vector 350→250 mb, averaged over Wiesbaden and Stuttgart under consideration of the stereo-measured 250 mb wind direction, is 338°, 6.2×10^{-3} sec^{-1}.

These shear directions call for an explanation of the band orientation, which will be given in chapt. 3.

The cirrus tops were at the level of the wind maximum (250 mb at Stuttgart and Wiesbaden, Fig. 13). This is in agreement with the theory of KUETTNER [11]. The value $\frac{\partial^2 u}{\partial z^2}$ as determined for the 300→200 mb wind profile was $-1.3 \times 10^{-5} m^{-1}$ sec^{-1} at Stuttgart, $0.7 \times 10^{-5} m^{-1}$ sec^{-1} at Wiesbaden. The mean of both is fairly compatible with the order of -1.0×10^{-5} m^{-1} sec^{-1} as postulated by KUETTNER [11]. Since in the present case the relative wind from 300 up to

200 mb well oriented parallel with the general wind direction -- especially at Stuttgart, which must be considered best representative -- it was possible to underlay u instead of u_r in determining this profile gradient.

2.1.2. Surface weather.[1] A marked High ridge extends from Finland southward over eastern Germany to the western Mediterranean, with a weakening High cell located over Bohemia.

Darmstadt is at the western flank of this High. East of Iceland a Low moving toward northeast causes an advection of warm air toward Scandinavia. A central Low is located northwest of the Azores. A comparison of the 6:00 surface weather with that of 15:00 (Fig. 8) shows no noticeable change over western Europe.

Surface temperatures, like the high level temperatures, steadily increase toward west. However -- with the sole exception of Scotland and northern Scandinavia -- no surface front exists over central Europe.

2.1.3. High level synoptic situation. The temperature distribution in the troposphere causes an inclination of the pressure centers towards west (compare Figs. 8 and 9: The Low near Iceland, the cold Low over SE Europe and the High ridge which in 300 mb extends from Spain towards the northern Baltic Sea. Between this High ridge and the cold Low over Yougoslavia there exists a jet stream, some 4000 km in length. At its warm (right) side, a cloud cover which exclusively consists out of cirrus, increases toward west (Fig. 2).

The ci-bands over Darmstadt -- some 230 km west of the jet axis -- are part of this ci-cover. They are located in the large, northwestern entrance-zone of this jet (Fig. 9). In the area of the jet axis the sky is completely clear (Fig. 2). The isonephs are quasi-stationary, at least within the period from 9:00 till 15:00. This must, partly at least, be attributed to the fact that the jet stream axis has no considerable east or west component of migration; the same can be expected to be true for the "jet front" (Fig. 16).

[1] This and subsequent chapters up to 2.1.7. were composed by Dr.K.WEGE.

The direction of the jet axis is from 15° to 195°, it crosses the contours from higher to lower pressure. The ci-bands (Figs. 1,2,3) and isohumids (Fig. 14) are nearly parallel with the jet axis. There is small positive acceleration of the air parcels in this area.

Horizontal wind shear over Darmstadt: 11 kn/100 km = 5.5×10^{-5}/sec*) which implies dynamic stability. Slight cyclonic curvature of the contours. As mentioned above the ci-bands as well parallel the isotherms (Figs. 10,11, 12). The horizontal temperature gradient is directed toward west in 300 mb and toward east in the 200 mb level (temperature compensation in the stratosphere). The ci-level still resembles the temperature distribution of the troposphere; this is shown by the temperature observations in 250 mb over Emden (-60° C) and Berlin (-64° C). In accordance with the temperature distribution the tropopause declines toward east, and the line of intersection of tropopause and 200 mb level runs parallel to the jet axis from north to south (Fig. 12), thus the ci-bands are perpendicular to the slope of the tropopause.

2.1.4. Stability. The thermal stability within the cirrus layer (and little below), 250/300 mb over Stuttgart at 14:00 is expressed by the mean vertical gradient of temperature, $\gamma = -\frac{\partial T}{\partial z}$[°C/100 m]. It was 0.80°/100 m; at the top of the ci it suddenly decreased to 0.58°/100 m.

2.1.5. Temperature advection and vertical motion. The value $\left(\frac{\partial T}{\partial t}\right)_{adv}$ (see Appendix) was determined for the layer 200/300 mb, its thickness being Δz. It yields $\left(\frac{\partial T}{\partial t}\right)_{adv} = -1.55 \times 10^{-4}$[°C/sec] = -6.7°/12 hours. This represents an instantaneous value which apparently by far exceeds the true value.

The large scale vertical motion near 300 mb as computed for an air parcel travelling from the Skagerrak to Stuttgart is $w_{12} \approx 0$. A comparison with the temperature analyses suggests that over northern Germany a slight ascending motion prevails, while over southern Germany slight subsidence takes place (compare with paragr. 2.1.7.). The ci clouds were probably generated in the area of the High ridge. On the other hand chapt. 2.2. suggests superimposed small scale vertical motions organized in bands.

*) If the horizontal wind shear does not approach the indifferent stage, it was computed in a pressure and not in an isentropic level.

2.1.6. Humidity. There were no measurements of humidity in the ci layer. The highest observation (300 mb) yields no ice saturation.

2.1.7. Vorticity advection was negative over Darmstadt, but positive over northern Germany (Fig. 19). This affirms the comments made in paragr. 21.5. on the vertical motion.

2.2. Small scale motion.

As already mentioned in chapt. 2.1. four bands which passed close to Darmstadt (Fig. 7) were spaced 14, 8, 6 km as measured east to west. A comparison with additional photographs, not shown here, demonstrated that the large band of Figs. 1,2,4,5,6 is the same as that at outer right of Fig. 7a. Still west of it, a fifth band is hinted (point O in Figs. 1,3; point E in Figs. 4,5a; Fig. 6). Although it is not pronounced traces are marked sufficiently as to affirm that a -- perhaps supressed -- banding took place. With this band distant from the more pronounced band by 7 km, the total of spacings which could be measured with reasonable accuracy of band identification becomes 14, 8, 6, 7 km, as measured east→west. This roughly represents a regular spacing and, as such, suggests the existence of a small scale motion organized to the effect of lift under the ci-bands, while subsidence would take place in the clear air "bands" between the ci-bands.

To the extend that "cells" as arranged along the band axes could be identified, their mean distance as measured along the band axis in Figs. 3,5a,6,7a was 1.2 ± 0.2 km (where the standard deviation is that of the individual distance, not that of the mean distance). It has to be emphazised, however, that these values refer to areas where cells were arranged somewhat regular.

On grounds of the single pictures taken from 11:43 till 11:50, the lateral motion of 8 wing tips of the approaching bands was measured. This motion toward both sides of the band axis averaged 0.9 ± 0.3m/sec each; it was hence nearly symmetric.

Fig. 5b shows a portion of the band with motion vectors in a coordinate system fixed with respect to the mean motion of points which are located close to the band axis. Due to great difficulties in

precise stereo identification of cloud points in subsequent photographs errors up to 0.2 m/sec may be superimposed on these vectors (as to both amount and direction).

The band topography (Figs. 5a,6) hardly offers a hint that the "wings" would be part of a helical trajectory. Perhaps, however, a helical motion had existed earlier which might nearly have ceased when the stereo photographs were taken; a flattening of the cirrus topography might in the meantime have taken place.

Some waves with $\lambda \approx 0.25$ km are indicated in the wings at 12:40 (upper right portion of Fig. 7a). This demonstates the existence of shear in very small scale, most probably confined to very shallow, stable layers; this shear can hence not affect large scale banding.

3. Discussion.

3.1. The present case of ci-bands near 260 mb is in fair agreement with the scheme advanced by CONOVER [6]: They are located in a zone of entrance, at the right side of a long jet, and nearly parallel with the latter as to their orientation. The high level front in this case, -- as opposed to case I -- approximately parallels the wind direction. - Band data are also compatible with $\Delta\alpha(\omega)$.

3.2. Ci-bands were parallel with large-scale 300 mb-isotherms and with isonephs; the latter, over Germany, consisted almost entirely out of cirrus, and were nearly parallel with the 400 mb isohumids (Figs. 2, 14).

3.3. Vertical wind shear as determined from the wind soundings is apparently not very representative as to time or position. This is suggested by the fact that closer to sounding time, random masses of cirrus prevailed.
Rounding off wind direction values to 10^0 units also has great influence on shear direction in this case since the latter is roughly parallel with the wind.
Thus, for the 250 mb wind direction, equal to 0^0 according to all the sounding stations in question, a slight correction of 4^0 has to be applied, according to the photogrammetrical measurement of cloud motion.
The true shear vectors of the relative wind which generated these bands is then certainly approximated by the following assumption : 350→310 mb : 340^0, $4\text{x}10^{-3}$ sec^{-1} ; 310→275 mb : 0^0, $12\text{x}10^{-3}$ sec^{-1} (this shear is anticipated to have brought about the bands at 260 mb); 275→260 mb : 320^0, $6\text{x}10^{-3}$ sec^{-1} (this shear apparently produced the fallstreaks pointing toward NW, Figs. 1, 3, 5).
Whether this relative wind or the Stuttgart wind is taken, a value $\partial^2 u_{(\omega)}/\partial z^2 \approx 1 \times 10^{-5} m^{-1} sec^{-1}$ results by both -- in agreement with the amount predicted by KUETTNER [11]. The bands again are close to the level where $\partial u/\partial z = 0$.

3.4. The spacing of these ci-bands was close to regular, with some 7 km as a rule. In case that the (spacing/thickness)-ratio would be roughly 3 -- as that obtained in case I -- , the shearing layer, reaching from the lower boundary of strong shear up to band tops, should be 2.3 km. It is not quite clear upon the wind soundings whether this was the case; if the level of the jet front (Fig. 16) is anticipated as the lower boundary, a thickness of 2.5 km up to the band tops would result. In this case, the assumption made above (3.), concerning the actual shear which generated these bands, is not complete.

5. Small scale lateral motion within "wing tips" was in fair accordance with similar results earlier obtained by CONOVER [6].

case study III: 6 Nov. 1962

1. Introduction.

Stereo pairs of this case were taken at one-minute intervals from 14:14 till 14:24. The photogrammetric base, located in Darmstadt, was 1.725 m in length, oriented $65^{\circ} \leftrightarrow 245^{\circ}$.

Cirrus clouds which were close to random masses in appearanc occurred at three different levels.

The orientation of the streaks across their direction of motion reflects a case of isotherms which cross the contours (of the same level) at considerable angle. It was caused by the area in front of a high level cold air "tongue" which intensified in the course of the subsequent 20 hours (compare Fig. 7, and Fig. 10 of case IV), creating more pronounced bands in the rear of this "tongue" on the next day (case IV). It is this circumstance which justified to report this case study.

2. Cirrus properties and meteorological conditions.

The cirrus of this case mainly occupied three different levels which incidently, differ by 1.1 km each: A band or rather streak composed of cc and fall-streaks (system A,B) at 7.1 km; two streak systems, C,D and E,F, at 8.2 km; and a portion of a cc-layer with its base at 9.2 km while the tops slightly exceed 9.5 km (Fig. 1).

Motion vectors and resulting mean vertical shear were inscribed in Fig. 1 (magnified below). Evidently, vertical wind shear did not exceed 3×10^{-3} sec^{-1}, at least not throughout layers of 1 km thickness. As a consequence, no large scale banding could take place: The streak lengths were in the order of 10 to 20 km.

In a similar case ([20], 8 Oct.1958), ci-streaks of lengths in the order of 10 km formed at four different levels; they also paralleled the respective shear, the amount of which was in the order of 6×10^{-3} sec^{-1}, and were also topped by a cc-layer. While their shear was greater, the thermal stability of the layer in which they occurred (200/300 mb), if expressed in terms of $\frac{\partial \theta}{\partial z}$, was more than twofold. Therefore, the two cases are accompanied by approximately the same RICHARDSON number.

All of the more pronounced streaks paralleled the wind shear at

and/or slightly below their level. This is described in more detail under the following chapter.

2.1. Wind conditions.

The wind vectors at the three cloud levels, as determined by cloud motion measured in the stereo pairs, agree well with the cross section[1] (Fig. 11). The cirrus occurred in an area of minimum wind between two jet axes (Figs. 5,6,11).

According to the Stuttgart soundings, the mean vertical shear 400 → 300 mb is 105°, 4.1 x 10^{-3} sec^{-1} at 12:00, decreasing to 130°, 3.0 x 10^{-3} sec^{-1} towards 18:00. The mean shear in the same layer at Darmstadt, (between vectors I and III, points A and G, Fig. 1), is only 140°, 1.7 x 10^{-3} sec^{-1} at 14:14.

The streaks at 8.2 km evidently are governed by the mean shear $\overrightarrow{\text{I II}}$, which is 100°, 2.8 x 10^{-3} sec^{-1}. Some faint ci-streaks in the foreground of Fig. 2b, at ≈8 km, which become visible only by stereoviewing, have this same orientation.

A few cc-streaks at outer left of the photograph, depicted larger in Fig. 2a, 14:08, display an orientation (dash-stippled) which exactly parallels the mean shear $\overrightarrow{\text{II, III}}$.

Concluding from the pointing of fall streak ends, the streak of 20 km length was produced by a shear of opposite direction (approx. 250°). However, it is established that neither direction nor amount of these high level winds would permit the formation of a large scale vertical wind shear.

2.2. Surface weather development[2].

The weather situation is characterized by a central Low over the Biscaya and a blocking High over European Russia (Fig. 4). Between both, a front between different air masses lies across Germany in NW↔SE orientation (compare also Fig. 11); (it is pronounced merely at higher levels).

This "front" passed Darmstadt at noon. West of it weak, east of it stronger southeastern surface wind prevailed. A stow of winds at lower levels is caused by the Alps.

---

[1] On account of the time difference between upper air soundings and the cirrus observations, none of the stations downstreams from Darmstadt was used for the construction of the cross section.

[2] chapters 2.2 through 2.7 were composed by Dr.K.WEGE.

2.3. High level synoptic situation.

The Biscaya central Low reaches up to the lower stratosphere, migrating very slowly toward SE. The anticyclone over Russia is linked with a strong, meridional High ridge. Between both, a southeastern flow is induced. Within this flow, the above mentioned high level cold front is linked with a jet stream over France. A second jet extends from Hungaria to the North Sea.

The cirrus measured in Darmstadt were located some 500 km northeast of the southwestern jet axis, and some 300 km southwest of the northeastern jet axis in a wind minimum. Both jet axes cross the band orientation at an angle of roughly 50°. There was little horizontal wind shear, no significant acceleration of the wind, and cyclonal contour curvature over the Darmstadt area.

The temperature distribution in the upper troposhere (Figs. 7,8) over Darmstadt was characterized by isotherms nearly parallel with the ci streaks (Fig. 1), with the temperature increasing towards north.

2.4. Thermal stability.

Throughout the layer 280/420 mb, in which all of the three ci systems occurred, the vertical temperature gradients were rather steep ($0.8 \leqslant \gamma < 1.0°$/100 m; Figs. 12,13). These amounts correspond to little stability. Stereo viewing of the cirrus over Darmstadt in 300/400 mb reveals that some disorganized turbulence took place especially between 290 and 330 mb.

Within 12 hours (12 to 24:00) the temperature at the level of the lowest ci (near 400 mb) cooled by approximately 1.5° C, while it cooled by -2.7° C in higher levels, thus increasing the vertical temperature gradient.

2.5. Temperature advection and vertical lift.

of the 300/400 mb layer was: over Munich : 0 ;
over Stuttgart: -1.7×10^{-4}°C/sec (= -7.4°/12 hours)

For the 350/450 mb and 250/350 mb layers of Stuttgart, -0.54×10^{-4}°C/sec (= 2.3°/12 hours) and -1.6×10^{-4}°C/sec (= -6.9°/12 hours) were obtained respectively.

In 400 mb (Figs. 5,7), advection of cold air took place in accordance with the wind and the change in temperature as measured over Stuttgart. $v\nabla T$ yields 0.35×10^{-4}°C/sec (= 1.5°/12 hours), which is little less than the $v\nabla T$ value obtained obove for the 350/450 mb thickness layer $\left[\left(\frac{\partial T}{\partial t}\right)_{avd}\right]$. The actual temperature change at 400 mb as averaged of Munich (-1.3°), Stuttgart (-1.5°), and Köln (-3.7°) is -2.2°/12 hours. Thus the actual cooling exceeds the values which could be expected upon advection. This means that an ascending motion must have caused the excess cooling and the isentropic levels migrating faster than the wind.

From these data, w_{12} = +0.9 cm/sec results; substituting $v\nabla T$ by $\left(\frac{\partial T}{\partial t}\right)_{avd}$ yields $w_{avd} \approx 0$.

At <u>300 mb</u>, south of the cold air located over the Alps, warm advection occurs, while north of it (compare with $\left(\frac{\partial T}{\partial t}\right)_{avd}$ at Stuttgart!) cold advection takes place. Since Munich is located within the axis of the cold air, $\left(\frac{\partial T}{\partial t}\right)_{avd} = 0$ is confirmed (Figs. 6,8).

Since an air parcel which arrives at Darmstadt after 12 hours of travel, has had to cross this area of cold air, the 12 hours mean $v\nabla T$ may not be compared with $\left(\frac{\partial T}{\partial t}\right)_{avd}$ over Darmstadt.

From the vertical velocity with a mean temperature change $\left(\frac{\partial T}{\partial t}\right)_{12}$ of -2.4°/12 hours (Stuttgart -2.7°, Munich -1.6°, Köln -2.8°) w_{12} = +2.7 cm/sec results. But north of the cold air area a value for $v\nabla T = 1.4 \times 10^{-4}$°C/sec results. This equals the $\left(\frac{\partial T}{\partial t}\right)_{avd}$ value obtained for the highest ci-layer from the winds measured over Stuttgart (the latter seems to be a little too great). A comparison with the temperature change yields a slight subsidence in 300 mb north of the Alps. For a trajectory reaching from the Alps to the east cost of England, we obtain w_{12} = -0.4 cm/sec, whereas south of the Alps the considerable value of w_{12} = 4.4 cm/sec results; here cooling took place despite warm air advection! - The above mentioned air parcel with its terminal over Darmstadt, which yields a mean w_{12} = +2.7 cm/sec, was lifted only south of the Alps, while north of them it underwent a descending motion.

<u>Summarizing</u> we can state about the field of vertical motion: South of the Alps there was slight ascending motion in the lower ci-layer; in the higher ci-layers there was considerable ascending motion south of the Alps, while north of them slight subsidence took place. Therefore, we have to assume that the ci were generated

south of the Alps, and the subsidence was not large enough to bring the relative humidity from water to ice-saturation (see next chapt. and case V). The horizontal distance of the zero line of vertical motion is about 300 km.

2.6. Humidity.

The Munich sounding yields a relative humidity of 102 to 112 % over ice in the ci-layer, Köln very strong over-saturation (120 to 140 % E), whereas over Stuttgart no ice-saturation was observed (Figs. 12,13).

2.7. Vorticity advection.

With the computed vertical velocities (chapt. 2.5.) we can assume a zero level of vertical motion (combined with horizontal divergence) between 400 and 300 mb. The chart of relative vorticity shows that the assumption of FRENCH and JOHANNESSEN, that the 300 mb level lies below the zero level, is not applicable on this case. If we assume the zero level between 300 and 400 mb, then indeed subsidence by positive vorticity advection (Fig. 14) in 300 mb and ascending by positive vorticity advection in 400 mb over the area of Darmstadt is obtained. (The relative vorticity distribution in the 400 mb level is very similar to that in 300 mb).

3. Discussion.

(1) In view of the comparatively slow motion of these ci streaks, the great angular deviation of their orientation from their motion direction, $\alpha \sim 80^{\circ}$, is permitted by the $\Delta\alpha$ ($|u|$) statistics. It should also be noted that this case of angular deviation occurred, again, near a High ridge.

(2) The streaks roughly oriented parallel with isotherms, vertical shear and high level isonephs.

(3) Since vertical shear amounts, as averaged over 1.0 km thickness, in none of the high level altitudes exceeded 3.0×10^{-3} sec^{-1}, no large scale bands were able to form.
Small scale bands or streaks, present at all of the three levels, may have been due to greater vertical shear amounts, as averaged over more shallow layers.

(4) Humidity was close to ice saturation. In view of a subsidence of only 0.4 cm/sec which should be regarded as a mean over area and time, local areas of ascent -- in statistical distribution perhaps -- cannot be excluded to have existed.

case study IV: 7 Nov. 1962

1. Introduction.

A few single photographs were taken between 8:22 and 8:30 in Ober-Ramstadt (Figs. 1,2,4).

At 10:50, a large field of not very bright ci-bands was sighted in Darmstadt; stereo pairs were taken from 11:15 from a base 1.73 km in length with the taking axis tilted by 45° toward east --hence pointing toward 21° (see map of Fig. 6). Ci-bands occurred at two different levels, some 1.5 km apart. Their orientation is cross the wind, thereby reflecting the existence of a high level cold air tongue which lay cross the contours.

The evaluation of these stereo pairs proved to be extremely difficult (1) due to the great distance of the bands from the base line and (2) because they lie almost parallel to the x'-axis in the pictures. As earlier described [20], this causes great relative mean errors in the horizontal parallax $p_{x'}$. Additional methods of measurement including vertical parallaxes caused by the horizontal tilt were employed in order to attain the required accuracy.

At 14:20, low mammatus were observed as they deformed into streaks -- toward 15:00 -- under an apparently strong vertical shear.
At 15:30, drizzling rain set in.

2. Ci-band properties and meteorological conditions.

(1) Bands photographed at 8:30 (Figs. 1,2,4) were estimatedly at 8.0 km[1] in agreement with measurements of their motion vector and the wind vector at Stuttgart; their motion vector was 210°, 28 m/sec; they were oriented 150°↔330° (see map of Fig. 3). The length of these bands was at least 150 km, the spacing of four different bands (in Fig. 1, measured from SW to NE) being 7.0, 6.5, 6.5 km. Bands which were photographed a few minutes later (Figs. 2,4) were spaced -- less regularly --: 9, 7, 6, 5 km, also measured SW to NE. This irregularity may only partly be attributed to measurement deficiency.

(2) Bands photographed at 11:00 (Figs. 5,6) lay at two different levels:

(a) The mean altitude of the system A,B,C,D,P,F was at 8.1±0.3 km (the second value denotes standard deviation of measurement

[1] According to estimates of the Bismarckturm weather station near Darmstadt.

errors); the bands oriented 114°↔294° moved 230°, 23 m/sec. The length of these bands was at least 220 km, their spacing was roughly 15 km (Fig. 6).

(b) The system G,H,I,L,M,N[1] was at 9.6±0.4 km, moving 225° ± 4°, 25 ± 3 m/sec, with an orientation 130°↔310°. The lengths of these ci-bands may be estimated also to exceed 150 km. The normal distance between systems H,I,K and L,M,N was some 40 km. All of these ci-bands roughly parallel the 400 mb and 300 mb isotherms (Figs. 9,10,11), as well as the isonephs at 9:00 and 12:00 (Fig. 16).

The tiny point z and neighboured cloud spots at 9.0±0.1 km vanished some 15 minutes after birth; their motion vector was 225°, 27 m/sec.

2.1. Wind conditions.

These ci-bands, in a manner similar to those of case III, also occurred in an area of relative minimum wind between two jet axes (Figs. 8.14). The wind vectors at all three levels where clouds were encountered agree with the cross section (Fig. 14) in which rawin measurements are summarized.

The most striking feature of the 12:00 hodogram is the strong shear 400→300 mb at Köln, Stuttgart, and Munich (Fig. 13).
The mean vertical shear 400→300 mb at 12:00 is over

Köln : 256°, 7.4×10^{-3} sec $^{-1}$;
Stuttgart: 262°, 11.3×10^{-3} sec $^{-1}$;
Munich : 262°, 8.4×10^{-3} sec $^{-1}$;
average : 260°, 9.0×10^{-3} sec $^{-1}$.

For Köln, the shear 462→339 mb should rather be considered; it equals 265°, 9.0×10^{-3} sec^{-1}. This shear vector can be considered the best representative for the ci-bands since on their travel downstream they came close to the latitude of Köln at 12:00.

The mean of the shear vectors of Köln and Stuttgart is 263°, 10.0×10^{-3} sec^{-1}, throughout a layer of some 1.9 km thickness.

---

1) By an apparent measurement error, the distance of this cirrus system is yet too near by 8 km in the drawing.

The maximum shear, of course, exceeds the average shear. Estimated by a profile of the relative wind, it attains some 17 x 10^{-3} sec^{-1}, at a level which is not quite 1 km below the level of the lower band system.

Although the three motion vectors could not be determined as reliable as to derive precise shear values, they still suggest that the mean vertical shear between the levels of the two large ci systems is not very great. This assumption is confirmed by the comparatively small shear at Köln, 339→300 mb -- covering the thickness between 8.2 and 9.1 km -- with 4.6 x 10^{-3} sec^{-1}.

According to the shear at Köln, Stuttgart, and Munich at 12:00 (Fig. 14), a thermal jet stream 400→300 mb, of very broad maximum, directed approximately along 270°→90°, lies over the area Darmstadt, Stuttgart, Munich (Fig. 13). While this shear maximum is lower at Köln (462→339 mb), it has finally shifted down to 500→400 mb at Wernigerode and Hannover, and thereby changed direction toward 290°→110°.

This remarkable arrangement deserves further attention: Like in case I, vertical shear is as strong and sufficiently extended in the horizontal as to enable that a lateral shift of the shear maximum to consecutive levels can be traced. However -- opposed to the far more common type represented by case I -- this downward shift does not occur towards the right, but towards the left of the shear vector direction! (i.e., the shearing layer slopes downward toward north). This implies that the cold air is not below, but above the layer of strong shear separating both air masses. This should explain why rather steep vertical temperature gradients, close to dry-adiabatic, occurred (see chapt. 2.4). The decline of this layer toward north is even slightly reflected in the levels of steepest lapse rate: While over Stuttgart and Köln it occurred roughly between 400 and 300 mb, it was between 500 and 370 mb at Wernigerode. A comparison with Figs. 9, 11 suggests that the center of the cold air within the layer 300/400 mb was roughly 100 km west of Hannover.

2.2. Surface weather development.[1)]

The cyclone which lay over the Biscaya on 6 Nov. has changed to the

[1)] chapters 2.2 trough 2.7 were composed by Dr.K.WEGE.

northwest cape of Spain on the morning of 7 Nov., while on the eastern coast of Spain another Low has arrived. In the course of the day, the latter cyclone migrates northward and joins the central Low over southwestern France. In the forenoon of 7 Nov., the faint high level cold front has reached the line Netherlands↔eastern Alps, where it diminishes. It marks the frontier between a weak southern flow in the west (maritime air) and a SE flow in the east (continental air).

2.3. Evolution of the high level synoptic situation.

A comparison of 300 mb charts of 6 Nov, 12:00, case III (Fig. 6) and 7 Nov., 0:00 and 12:00 (Figs. 7,8) demonstrates that an essential change took place in the flow regime of the upper troposphere: With a rapid migration of the alpine trough towards north, the jet, until then located over the western Mediterranean, moved to western Europe and the North Sea at 12:00. At its right side, a "jet finger" creates which points from the Rhone valley into northeast Germany. This caused a sudden change in high level wind direction from SE to SW over western Germany (Fig. 6 of case III, and Fig. 8 of this case). The pibal observations of Stuttgart and Köln at 06:00 (Fig. 12) and a comparison of Figs. 7 and 8 suggests that the trough passed Darmstadt at approximately this time.

It suggests itself that the 300 mb trough was associated with the high level cold air tongue, located over the Alps on the day before (see case III). Due to the position of the Darmstadt area in a relative wind minimum at 12:00, there was only little horizontal shear to the northwest, it was increasing up to 13 kn/100 km = 6.5×10^{-5}/sec (anticyclonal, dynamical stability). The horizontal distance to the main jet axis northwest of Darmst. was about 340 km; the distance to the jet finger southeast of Darmstadt about 120 km (Fig. 8). Darmstadt was located in the area of exit, the jet axes crossing the contours slightly toward higher pressure; there was negative acceleration of the travelling air parcels.

2.4. Thermal stability.

The high level thermal stability was essentially determined by the high level cold air (details of its properties were already described in chapt. 2.1.). Especially at the layer of the lower ci-bands, lapse rates close to dry-adiabatic prevailed (Figs. 16,17): It was $\frac{\partial T}{\partial z} = 0.85^{\circ}/100$ m at Köln, $\frac{\partial T}{\partial z} = 0.91^{\circ}/100$ m at Stuttgart. At the

higher ci layer, lapse rates were only 0.69°/100 m at Köln and 0.78°/100 m at Stuttgart. Both soundings display minor lapse rates below than above this cirrus.

2.5. Temperature change and vertical motions.

The temperature changes 0:00 to 12:00 over Köln (Stuttgart values in brackets) were: At the level below the lower ci (350 mb) -2.1°/12 hours (-0.5°/12 h), while it is -3.6°/12 hours (-0.5°/12 h) above that level. The cooling at Köln means an increase of the vertical gradient of actual temperature there.

Within the same time, the temperature change below the level of the upper ci system (close to 280 mb) is -3.6°/12 hours (-0.5°/12 h); above, it is $+1.8^{\circ}$/12 hours ($+1.1^{\circ}$/12 h).

This means cooling below, warming above this cirrus, hence a tendency toward stabilizing.

The temperature advection was determined upon the sounding of Köln: At the lower ci, for which the layer 300/400 mb was considered representative, $\left(\frac{\partial T}{\partial t}\right)_{adv} = +5.4 \times 10^{-4}$°C/sec (+23°C/12 hours, warm air advection); this value certainly exceeds the real value! Advection at the upper ci was determined for 210/310 mb, which yields -3.7×10^{-4}°C/sec (-16°C/12 hours, cold air advection). Since the backing of the wind, which yields the negative value for $\left(\frac{\partial T}{\partial t}\right)_{adv}$, does not begin below the tropopause, the value obtained above is not valid for the ci layer.

Vertical lift was determined merely upon $v\nabla T$, since $\left(\frac{\partial T}{\partial t}\right)_{adv}$ would yield no reliable values. Upstream of Köln, we obtain

at 400 mb, 0:00 till 12:00, $w_{12} = +2.3$ cm/sec;
at 300 mb, 0:00 till 12:00, $w_{12} = +3.1$ cm/sec;
12:00 till 24:00, $w_{12} = +1.9$ cm/sec.

Like on the day before (case III), ascending motion takes place in the same area with respect to the (northward migrating) cold air "tongue"; (i.e. in a "tongue"-fixed coordinate system the position of ascending motion does not change considerably in the course of 24 hours). From 0:00 to 12:00 the ascending motion mainly results from the local temperature decrease, whereas from 12:00 to 24:00 a temperature rise was observed which, however, was not as great as could be expected from the $v\nabla T$-values [see Appendix, (IV)].

2.6. Humidity.

Saturation with respect to ice was attained at Köln at 420 mb upward, increasing to supersaturation (with respect to ice) towards higher altitudes (400 mb: 105 %; 300 mb: 118 %; 255 mb: 130 %; Fig. 17). At Stuttgart, no saturation was attained close to 12:00. While a time decrease of humidity took place over Stuttgart, moist still increased at Köln.

2.7. Vorticity advection.

Since the 300 mb streamlines at 12:00 (Fig. 8) and the isopleths of the relative vorticity are nearly parallel, it is hard to decide whether positive or negative vorticity advection took place at 12:00.

3. Small scale features.

Close inspection of the bands in the area near point P in Fig. 6 suggests that vertical shear, directed in band orientation, prevailed through the band thickness. The vertical component may indicate existence of fall streaks.

Near the points H,I, six waves of equal lengths, 4.1 km each, could be identified. Their shape can be approximated by scetch (a); four minutes later, the shape had changed to (b)[1]. The vertical amplitude Δz as defined by (a), was 0.5 km.

AVSEC observed and described a phenomenon, equal to this in principle, upon one of his experiments; he wrote [1]:

"Our experiments, performed on a broader basis, permitted us to observe that these vortices resulted from a superimposition of two effects:

1. The spontaneous generation of transversal waves at the boundary which parts the upper clear air layer from the smoke below, as soon as their motion velocities become different.

2. The generation of transversal rolls of convective kind, whereby each pair of rolls (or billows) was located in a hollow which was formed by (and between) two neighboured wave crests."

AVSEC then describes the four different stages which these waves undergo.

---

1) These features were realized only when the Figures had been completed; hence no magnified photos of the different stages are included.

The waves depicted in Fig. 6 and nearby under (a) correspond to stage 2, while the shape depicted nearby under (b)[1] correspond to stage 3 of AVSEC's experiment.

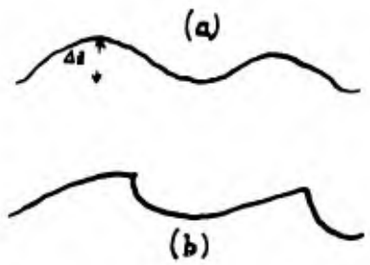

4. Discussion.

(1) Orientation of ci-bands differed by 60° and 64° from their respective motion direction. Since the respective velocities were 28 m/sec and 23 m/sec, these angles are yet compatible with the $\Delta\alpha(|u|)$ statistical law. The edge of an apparent layer not far below the tropopause deviated from this rule, according to the measurements, by some 18°. Since it was distant some 100 km it is suspected that this apparent deviation is, to a part, added up from errors in measurement of motion direction and velocity. It is moreover not certain whether these edges can be regarded as parts of large scale ci-bands, merely for which the $\Delta\alpha(|u|)$ has been regarded to be of validity *without exception*. The area of these ci-bands is not far from a large, extended High ridge.

(2) The lower ci-bands oriented parallel with the isotherms and the wind shear which dominated below and at band level. The precise levels of the ci, with respect to the relative wind profile, could not be determined. Yet there is no doubt that these bands were generated by strong, large scale shear.
The relative wind at Stuttgart and Köln, taken with respect to a coordinate system fixed with the 500 mb wind vector and in west↔east orientation, yields a profile which fairly well agrees with that described by KUETTNER [11].
The bands were also parallel with the isonephs near Darmstadt at 9:00 and 12:00, the underlying cloud cover consisting mainly out of cirrus.

(3) The fact that both vertical shear maxima and levels of steepest lapse rate shift to lower levels, toward the left of the shear direction, revealed the existence of a high level cold air mass compatible with the actual horizontal and vertical temperature distribution.

---

[1] see footnote on page 73.

In most of the cases, best represented by case I, the cold air is below the warm air, to the effect that the layer of strongest shear is also a layer of increased thermal stability.

Oppoced to this more common mode, however, the present case represents the contrary: Due to the overhanging cold air, the layer of maximum shear is also a layer of least thermal stability! This probably caused the bands -- at least the lower ones -- to generate still within the strong shear -- as both their altitude and appearance suggest.

case study V: 1 March 1963

1. Introduction.

Moderately pronounced ci-bands were photographed on this day from 9:40 till 13:49; stereo-pairs were taken from 10:46 through 13:51. Cirrus prevailed within the northern half of the sky over Darmstadt, while the southern half had little cloud amount; a diary note says that from 12:50 till the end of these observations the southern half of the sky was free of any clouds. Both position and/or little contrast of the band inhibit tracing of eventual small scale motions.

2. Cirrus properties and meteorological conditions.

During the period of measurement the band level was 9.5 km, with the tops at 9.8 km and fall streak bases at 9.0 km. The bands were at least 250 km in length.
The following table indicates details of the geometric data:

Table I:

Fig.No.	time	altitude km	band motion vector	band orientation	streak orientation
1	9:42	9	not meas.	--	--
2 (tow.SW)	10:03	9	not meas.	--	$80^{\circ} \leftrightarrow 260^{\circ}$
3	10:16	9	79°, 17 m/sec	$68^{\circ} \leftrightarrow 248^{\circ}$	short streaks varied $180^{\circ} \rightarrow 0^{\circ}$ to $200^{\circ} \rightarrow 20^{\circ}$
	11:28	9.2	83°, 19 m/sec	$74^{\circ} \leftrightarrow 254^{\circ}$	
	13:38	9.2	97°, 20 m/sec	(mean of 3 bands:) $89^{\circ} \leftrightarrow 269^{\circ}$	
	13:49	9.2	not meas.	$98^{\circ} \leftrightarrow 278^{\circ}$	

Ci-bands kept roughly parallel with isotherms and relative topography (thickness pattern) close to their level (Figs. 6,7,8), and isonsphs at 12:00 (Table I and Fig. 11).[In the present case, isotherms were difficult to determine since an only small horizontal temperature gradient prevailed in the large scale].

Small scale features of the observed bands were as follows: Three neighboured bands in Fig. 1e were spaced 14 km and 12 km, respectively. Between three bands of streaky appearance in the foreground of Fig. 2, 13:38, spacing was 13 and 5 km (the middle band was rather narrow). Finally, the distance between two bands in Fig. 2, 13:49, was roughly 14 km (the southernmost band is not completely visible). No halfway regular spacing was else recorded. Short streaks originating from the band in foreground of Fig. 2 (11:02, 11:28), fell toward north.

2.1. Local wind conditions.

To the extent to which wind conditions pertain to this cirrus field, they were characterized by a jet finger some 275 km SE of Darmstadt (Fig. 4); and by moderate wind shear in 300/400 mb directed nearly opposite the jet (Figs. 4,7, 9). It is suspected that a meso-scale thermal jet 300/400 mb, pointing toward 60°, lay over and slightly north of Darmstadt. Its mean shear amount can be estimated to 6×10^{-3} sec^{-1}, the maximum value naturally exceeding the mean. Over Stuttgart at 12:00, the 300/400 mb shear was 200°, 6.1×10^{-3} sec^{-1}; over Köln, the 300/380 mb shear was 260°, 5.0×10^{-3} sec^{-1}.

The 12:00 wind sounding of Idar-Oberstein, which shows no shear within this layer, seemingly contradicts this assumption. It is, however, a result of experience that in this sounding wind details were often evened out.

Since in the present case the radiosonde was carried still farther to the west by this wind, i.e. away from the Darmstadt area, the shear obtained in that area may indeed have had smaller amounts -- as Figs. 6,7 suggest --; but it was most probably not zero.

There is another indication that the band orientation was governed by 300/400 mb relative wind: As Table I indicates, the band orientation changed from $68^{\circ} \leftrightarrow 248^{\circ}$ at 10:16, over $74^{\circ} \leftrightarrow 254^{\circ}$ at 11:28, to $98^{\circ} \leftrightarrow 278^{\circ}$ at 13:50. This roughly approximates the tendency of successive orientations of the isotherms north of the warm air tongue when the latter moved WSW-ward SE of Darmstadt (with the general high level wind).

2.2. Surface weather situation.[1)]

Central Europe was covered with a stationary High centered over the Bescides (50°N, 20°E), which slowly weakened. A strong ridge of it stretched toward southern Scandinavia. The Darmstadt area is located at its western flank, in a cold low-level flow (Fig. 3).

2.3. Development of high level synoptic situation.

The High mentioned above reaches up to the 200 mb level; its axis is tilted toward northwest so that its upper center is located over the North Sea. Between this, and a high level Low over Yugoslavia, a jet extends from the Ukraine toward northern Italy. At its right side, a second jet axis extends from the Baltics to southern France. This jet axis lies some 275 km SE of Darmstadt, the ci-bands thus occurring at its right side; the ageostrophic wind component close to the cirrus area was evidently directed toward higher pressure; the air parcels hence decreased their velocity.

Horizontal wind shear is approximately 13 kn/100 km = 6.5×10^{-5} sec^{-1} (dynamic stability, despite anticyclonical shear). The direction of the jet axis and the band orientation differed by an angle of some 20°. Over the Darmstadt area, contours were slightly anticyclonal. Small temperature gradients prevailed at 300 mb at 12:00.

A cold air tongue stretched from the Baltic Sea westward to the Netherlands; a second cold air tongue stretched over the Alps. Between both cold air masses, a "ridge" of warm air extended toward WSW, the axis of which is south of Darmstadt. As a consequence of the small horizontal temperature gradients, analysis was difficult and in cases of uncertainty, had to rely on the vertical shear in the thickness pattern (rel. top.) 300/400 mb. The relative topography 200/300 mb finally compensates the Low over Yugoslavia, to the effect that the horizontal temperature gradient prevailing at this level is uniformly directed toward SSE. The tropopause is only slightly inclined, due to the small temperature gradients. The bands were some 1.2km below the tropopause.

2.4. Thermal stability.

Thermal stability will be determined upon the 12:00 sounding of Idar-Oberstein, located 100 km downstream of Darmstadt; corresponding

---

[1)] chapters 2.2 through 2.7 were composed by Dr. K. Wege.

values of the 06:00 sounding will be added in brackets (compare with Figs. 12,13):

$\frac{\partial T}{\partial z}$ = 0.86°C/100 m (0.80°/100 m) at 350/400 mb; and
0.76°C/100 m (0.80°/100 m) at 300/350 mb.

This corresponds to rather steep vertical temperature gradients. Both Stuttgart and Köln had a yet steeper lapse rate, with 0.87°/100 m throughout 300/400 mb.

2.5. Temperature change, advection and vertical motion.

According to the Idar-Oberstein soundings, the 6-hourly temperature change was between +1° and +2° below, at and above ci level. Over Köln, there was a 12-hourly increase of roughly 1° below, and a 1° decrease above ci level. The following values of temperature advection $\left(\frac{\partial T}{\partial t}\right)_{adv}$ were determined for the 250/350 mb layer

at Idar-Oberstein (12:00): +2.07 x 10^{-4}°C/sec (= 8.9°/12 hours);
at Köln (12:00): 0.0°C/sec.

Advection is subject to fluctuations as to both level and time. For instance, over Idar-Oberstein from 06:00 to 12:00, advection changes its sign both below and above cirrus level, whereby the (calculated) amounts of advection perhaps exceed actual advection. The high level synoptic situation over the Darmstadt area, including the nearby jet, implies that on the large scale and within greater time intervals, slight subsidence prevailed. We may draw the same conclusion if the humidity distribution is considered. Calculation employing conditions 12 hours upstream of Köln at 0:00 yields w_{12} = -0.6 cm/sec. Analogous calcualtion with conditions 6 hours upstream of Idar-Oberstein at 06:00 also yield w_6 = -0.6 cm/sec; here, however, $\nabla_H T$ had to be determined upon a 06:00 value obtained by interpolating between the 0:00 and 12:00 terms. The vertical motion as determined upon $\left(\frac{\partial T}{\partial t}\right)_{adv}$ would be w_{adv} = +2 cm/sec; this value certainly exceeds the actual value; this can be explained by the fact that the underlying $\frac{\partial T}{\partial t}$ term represents an instantaneous value. Analogous calculation yields for Köln w_{adv} = +0.1 cm/sec.

We must conclude that the observed cirrus field was of meso-scale extent, generated in comparatively narrow areas of ascent which were enclosed in a larger area of general subsidence. The network of sounding stations was apparently yet too wide-gridded as to yield results best representative for these cirrus.

2.6. Humidity.

The soundings of Idar-Oberstein (06:00 and 12:00), also of Köln (12:00),and Stuttgart (12:00) imply that there was no ice saturation (Figs. 12,13), despite cirrus amounts up to 4 eights near Köln at 12:00 (Fig. 11). Changes of humidity with time were small and within measurement errors. This is compatible with the large scale subsidence (see chapt. 2.5.).

2.7. Vorticity.

Vorticity advection at Darmstadt, 12:00, was negative both at 500 mb and 300 mb (Figs. 14,15).

3. Discussion.

3.1. The difference between band orientation and motion direction kept nearly constant at approximately 10°. This angle is far within compatibility with the velocity, considering $\Delta\alpha(|u|)$. A jet finger lay some 275 km southeast of these bands. A rough parallelism of bands with the former is certainly "incidental".

3.2. The fact that the shear 300/400 mb was nearly opposite the general high level wind, had a major share in causing these bands to move comparatively slow.

3.3. Bands paralleled isonephs especially at 12:00, It can be assumed that isonephs -- which entirely consist of cirrus amounts -- represent the local high level isotherm direction better than isotherms which were derived from actual temperature measurements. Sounding stations proved too sparse in this case as to account fully for the details.

3.4. The present cirrus occurred in a large scale area of subsidence. Lift, which might be anticipated to have occurred upstream of Darmstadt, upon the temperature analysis of 0:00, was not present

there, since the 12-hourly temperature change surmounts the one which should be expected upon advection (thus, at Posen [12-330]: w_{12} = -1.6 cm/sec; at Prague [11-518]: w_{12} = -0.8 cm/sec). Even if we consider the daily temperature change by radiation (+0.5°C), vertical motion still remains.

Case study VI : 14 Febr. 1964

1. Introduction.

Moderately pronounced ci-bands were observed and photographed on this day from 8:15 through 14:50. Since the photogrammetry group was not complete, stereo photographs could start not earlier than 14:40.

Bands were moderately pronounced mainly from 8 through 11 hours and again from 12:50 through 14:10. Between these two periods, bands of appearance close to random masses occurred. Past 14:30, only lower ci masses, with band structure still present only in the large scale aspect, were observed (Fig. 5).

Despite great probabilities in favor of the estimated band altitude as furnished by different sources and data, ultimate certainty was not attained without stereo measurement. Incidently, due to the complicated meso-scale weather situation, precise information on actual meteorological conditions could also not be obtained.

2. Cirrus properties and meteorological conditions.

The following table informs on some of the essential data of these ci-bands :

Table I :

Fig.	time	altit. [km]	orientation	motion direct.	motion veloc. [m/sec]	mot. dir. minus orientation
1 3b 3	8:15 8:30 8:45	8.3*)	127°↔307°	not meas.	very slow	
4a	9:30	8.3*)	127°↔307°	133°	4.8	5°
--	10:50	8.3*)	125°↔305°	134°	7.3	9°
--	11:50	8.3*)	127°↔307°	not meas.		-
4b	13:00	8.3*)	120°↔300°	136°	14.3	16°
5	14:40	5.8	109°↔289°	173°	3.7	64°

1) Synoptic charts for this case were made by Mr. R. MEISSNER.

*) Altitudes according to estimates of four different main weather stations; all other data were obtained by photogrammetry.

Motion and orientation of these bands changed very slowly and steady from 8:15 through 13:00. The abrupt change in motion direction toward 14:40 is certainly due to the change of cirrus occurrence to a far lower altitude.
These ci-bands paralleled the isotherms both of 400 and 300 mb (Figs. 7, 9); as well as the thickness pattern (rel. top.) 300/400 mb and the isonephs close to Darmstadt (Figs. 2, 10) -- the latter consisting almost entirely of cirrus; and also the 344/500 mb wind shear at Stuttgart (Fig. 11).

2.1. Wind conditions over southwestern Germany.

The thermal wind distribution was rather complicated in this case, with strong directional changes especially at 400 and 300 mb (compare Stuttgart, Darmstadt [Table!] and Köln, Fig. 11), so that the density of the network of sounding stations -- with a mean distance of some 100 n.mi. -- was not sufficient to explore fully the actual wind conditions. Hence no proper cross section was plotted. Winds at Köln and Stuttgart at 12:00 and 18:00 suggest that the eastward extending trough over France slowly moved northward (see chapt. 2.3). If it is considered that the radiosonde of Stuttgart had migrated some 10 km to NNE of Stuttgart when reaching the shearing layer, the distance normal to the bands observed SE of Darmstadt shrinks to some 50 km. This suggests that despite the great bend in wind direction, Stuttgart rawin measurements of 12:00 are yet the best representative.
At Stuttgart, 12:00, in the average from 500 through 344 mb (thickness of 2.6 km; Fig. 11), vertical shear was 103°, 5.0 x 10^{-3} sec^{-1}; maximum shear within this layer was greater, of course. The mean direction 500→400 mb coincides with the orientation of ci-bands encountered from 8 until 13 hours. The wind shear at Köln is negligible in comparison.
A strong argument in favour of the estimates of 8.3 km is the wind direction at 340 mb : If the Stuttgart value is given a greater weight -- as compared to Köln--, due to Stuttgart's location closer to Darmstadt, the resulting weighed mean of winds is 140°, 9 m/sec -- well compatible with the band motion direction. Whereas beyond the layer 300/380 mb every wind vector mean would yield directions which exceed 145°(comp. Fig. 11).
the 300→250 mb shear at Munich is roughly the same as that at Stuttgart; at Köln, however, it is opposite. This adds up to the assump-

tion that the layer above the high level ci-bands had smaller amounts of shear over Darmstadt than over Stuttgart.
Finally, the strong change of wind from 12:00 to 18:00 (Figs. 11, 12) should be noted; it is mainly caused by the northward migration of the strong jet stream over the alps at 12:00.

2.2. Surface weather conditions.

Darmstadt was located at the western side of a High over Hungaria. A front separating (low level) continental cold air in the east from warm maritime air in the west extended from southwest England over France to Italy. From the western Mediterranean there was advection of warm air toward northeast, increasing during the day as the result of a deepening Low which moved eastward over Spain. The obeserved ci-bands belong to the northernmost edge of the cloud system caused by this advection of warm air (see Fig. 2 and the end of chapt. 2.3).

2.3. High level synoptic situation.

At 0:00, a trough extended from the eastern Atlantic into France; a second, very intensive trough was located over western Russia, there causing a strong northerly high-level flow over eastern Germany. Between both troughs a High ridge extended with its axis a few km west of Darmstadt. A strong jet stream lay over Spain and the Mediterranean ; a second (weaker) one was over the British Isles at the northeastern side of the trough first mentioned.
In the course of the subsequent 12 hours the axis of the jet over the western Mediterranean shifted some 500 km northward -- as measured along the 5° E Meridian (Fig. 6). This shift was caused by the warm advection mentioned in chapt. 2.2. (see also the migration of e. g. the -50°isotherm in 300 mb, Figs. 8, 9). As a consequence of this development, the trough over France was slowly shifted northward, too, thereby extending slightly toward east. The jet over England migrated perpendicular to the direction of its axis, northeastward.
The position of the trough is well reflected also in the 400 and 300 mb temperature distributions: The tongue of cold air connected with the trough lies somewhat south of Darmstadt.
The axis of the High ridge at 12:00 lay east of Darmstadt, after having passed it in the early morning (see also Table I : ci-bands moved from SE with velocity increasing from about 9:00 on).
There was only small horizontal wind shear over Darmstadt, with

cyclonic curvature of the high level contours.

The cloud cover over northeast Germany consisted mainly out of low clouds, while in the south and west of Germany cirrus prevailed (Fig. 2).

Cirrus altitude and amount estimates were

at Karlsruhe : 8.3 km , 6/8 ci spiss and cistr, 8:00 - 11:00, with only 1/8 left at 13:00; no ci after this term

at Mannheim : 8.3 km, 5/8 ci fib, unc, 8:00 - 13:26;

at Stuttgart : 8.3 km, 3/8 ci, 8:00 through 15:00

at Köln : 6.1 km, 3/8 - 5/8 ci, 9:30 - 15:30.

2.4. Temperature advection and vertical velocity.

The ci-bands probably occurred near the 350 mb level; above it, the wind (at Stuttgart) was backing; below, veering winds prevailed. This means that there was cold advection above , warm advection below ci level (increasing lapse rates !). Therefor, $\left(\frac{\partial T}{\partial t}\right)_{adv}$ was computed separately, each for a layer above and below the cirrus level, upon the Stuttgart sounding of 12:00 :

250/344 mb : $\left(\frac{\partial T}{\partial t}\right)_{adv} = - 1.48 \times 10^{-4}\ ^{o}C/sec = - 6.4\ ^{o}/12\ h$

344/462 mb : $\left(\frac{\partial T}{\partial t}\right)_{adv} = + 1.12 \times 10^{-4}\ ^{o}C/sec = + 4.8\ ^{o}/12\ h$

Since the ci-bands were centered within the 300/400 mb layer, the mean $\left(\frac{\partial T}{\partial t}\right)_{adv}$ value was also computed for this layer :

300/400 mb : $\left(\frac{\partial T}{\partial t}\right)_{adv} = - 0.23 \times 10^{-4}\ ^{o}C/sec = - 1.0^{o}/12\ h.$

In the area of Darmstadt and upstream, there was rising motion of $w_{12} = + 3.3$ cm/sec (at 300 mb, 0:00 - 12:00), as compared to $w_{adv} = + 0.8$ cm/sec.

2.5. Vorticity.

Vorticity advection at 12:00, 300 mb (Figs. 6, 15) was nearly indifferent in the area of Darmstadt.

2.6. Humidity.

A survey of dew point differences at all significant levels showed that Stuttgart had the least humidity of all West German stations at 700 mb, while it had the greatest humidity of all these stations through the layer 250/500 mb. It is however still below ice saturation, according to Fig. 13.

2.7. Small scale features.

Individual cloud points on the "wings" and on the band axis could be traced in two subsequent photographs taken nearly toward zenit (Fig. 3). Eight cloud points located at or close to the "wing tips" fled to each side from the band axis with a mean of 0.5 m/sec. The man width of this band, i.e. the distance of the "wing tips" at opposite sides from each other, was roughly 1.5 km.

Stereo evaluation of pairs taken at 14:40 yields the following : (Fig. 5): Vertical shear between a layer cloud at 5.3 km and a system of bands and streaks at 5.7 km roughly parallels the latter. The shear vector 5.7→6.2 km, in turn, approximately parallels thin streaks at level 6.2 km. More precise measurements of motion vectors were not possible in this case due to both slow cloud motion and convective activity, by which point identity is lost quickly.

67

References

[1] D. AVSEC, Tourbillons thermoconvectivs dans L'Air; Thèses presentées à la Faculté des Sciences de L'Université de Paris, Octobre 1939.

[2] W. BUSCHNER, Zur Auswertung von Satelliten-Wolkenaufnahmen: Ein Wolkenwirbel als Kaltlufttropfen. Met. Rundschau 16, 4/1963, 123 - 126.

[3] D. BRUNT Patterns in ice and cloud. Weather, Oct. 1946, 184 - 185.

[4] H. CLAYTON, Discussion of the cloud observations. Ann. Astr. Observ., 1896, Harvard Coll. 30, 465.

[5] L. CLEM, Clear air turbulence near the Jet Stream maxima. Bull. Amer. Meteor. Soc. 36, 1955, 53.

[6] J.H. CONOVER, Cloud patterns and related air motions derived by photography. Harvard Univ., Blue Hill Met. Observ., Final Rep., Contract No. AF (604)-1589, June 1959.

[7] J.H. CONOVER, Cirrus patterns and related air motions near the jet stream as derived by photography. J.M. 17, 1960, 532 - 546.

[8] J.H. CONOVER, Cloud interpretation from satellite altitudes. GRD Research Note 81, AFCRL-62-680: Bedford July 1962.

[9] J.E. FRENCH, K.R. JOHANNESSEN, Forecasting high clouds from high-level constant pressure charts. Proc. Toronto Met. Conf. 1953; AMS and RMS 1954, 160 - 171.

[10] H. KOSCHMIEDER, J. REUSS, Empirical Results on the geometry of cirrus bands as related to meteorological conditions. Techn. Rep. No.1, under contr. AF 61 (052)-620, 118 p.; Darmstadt, April 1963.

[11] J. KUETTNER, The band structure of the atmosphere. Tellus 11, 1959, 267-294.

[12] F.H. LUDLAM, R.S. SCORER, Cloud study, a pictorial guide. London (John Murray) 1957, 1958, 1960.

[13] F.H. LUDLAM, L.I. Miller, Research on the properties of cloud systems. Final Rep. under contr. AF-61(514)-1292; London, March 1959.

[14] J.S. MALKUS, H. RIEHL, C. RONNE, W.S. GRAY, Cloud structure and distribution over the Tropical Pacific, Part II. Unpublished manuscr., Ref.No. 61-24 Woods Hole Ocean. Institution, August 1961.

[15] V.G. PLANK, Cumulus convection over Florida - a preliminary report; in: C.E. ANDERSON, Cumulus Dynamics, New York 1960.

[16] H.A. PANOFSKY, The effect of vertical motion on local temperature and pressure tendencies. BAMS 25, 1944; 271 - 275.

[17] H.A. PANOFSKY, Methods of computing vertical motion in the atmosphere. JM 3, 1946; 45 - 49.

[18] H.A.PPANOFSKY, Large scale vertical velocity and divergence. Comp. Met., AMS, Boston 1951; 639 - 646.

[19] R.R. REITER, Meteorologie der Strahlströme (Jet Streams), Wien 1961, 23 f.

[20] J. REUSS, Cirren in vertikaler Windscherung. Beitr. Phys. Atmos. 36, 1963, 173-188.

[21] J. REUSS, A contribution on the geometry of cirrus bands as related to meteorological conditions. Techn. Rep. No.2, contr. AF 61(052)-620; Darmstadt, Aug 1963

[22] J. REUSS, Die geometrische Gestalt von Schichtwolken als Merkmal der thermischen Winde ihres Höhenbereichs allgemein sowie der Windrichtung bei großer Windgeschwindigkeit. Abschl. Ber. an die DFG; Darmstadt, April 1964.

[23] R.S. SCORER, Theory of waves in the lee of mountains. QJ 75, 1949, 41 - 56.

[24] R.S. SCORER, verbal communication, April 1961.

[25] Z. SEKERA, Helmholtz waves in a linear temperature field with vertical wind shear. JM 5, 1948 ; 93 - 102.

[26] A. SPRUNG, R. SÜRING, Ergebnisse der Wolkenbeobachtungen in Potsdam und an einigen Hilfsstationen in Deutschland in den Jahren 1896 und 1897; Berlin 1903.